

# Determination of Earth's Transient and Equilibrium Climate Sensitivities from Observations Over the Twentieth Century: Strong Dependence on Assumed Forcing

Stephen E. Schwartz

Received: 20 July 2011 / Accepted: 20 January 2012 / Published online: 4 May 2012  
© Springer Science+Business Media B.V. (outside the USA) 2012

**Abstract** Relations among observed changes in global mean surface temperature, ocean heat content, ocean heating rate, and calculated radiative forcing, all as a function of time over the twentieth century, that are based on a two-compartment energy balance model, are used to determine key properties of Earth's climate system. The increase in heat content of the world ocean, obtained as the average of several recent compilations, is found to be linearly related to the increase in global temperature over the period 1965–2009; the slope, augmented to account for additional heat sinks, which is an effective heat capacity of the climate system, is  $21.8 \pm 2.1 \text{ W year m}^{-2} \text{ K}^{-1}$  (one sigma), equivalent to the heat capacity of 170 m of seawater (for the entire planet) or 240 m for the world ocean. The rate of planetary heat uptake, determined from the time derivative of ocean heat content, is found to be proportional to the increase in global temperature relative to the beginning of the twentieth century with proportionality coefficient  $1.05 \pm 0.06 \text{ W m}^{-2} \text{ K}^{-1}$ . Transient and equilibrium climate sensitivities were evaluated for six published data sets of forcing mainly by incremental greenhouse gases and aerosols over the twentieth century as calculated by radiation transfer models; these forcings ranged from 1.1 to  $2.1 \text{ W m}^{-2}$ , spanning much of the range encompassed by the 2007 assessment of the Intergovernmental Panel on Climate Change (IPCC). For five of the six forcing data sets, a rather robust linear proportionality obtains between the observed increase in global temperature and the forcing, allowing transient sensitivity to be determined as the slope. Equilibrium sensitivities determined by two methods that account for the rate of planetary heat uptake range from  $0.31 \pm 0.02$  to  $1.32 \pm 0.31 \text{ K (W m}^{-2}\text{)}^{-1}$  ( $\text{CO}_2$  doubling temperature  $1.16 \pm 0.09$ – $4.9 \pm 1.2 \text{ K}$ ), more than spanning the IPCC estimated “likely” uncertainty range, and strongly anticorrelated with the forcing used to determine the sensitivities. Transient sensitivities, relevant to climate change on the multidecadal time scale, are considerably lower,  $0.23 \pm 0.01$  to  $0.51 \pm 0.04 \text{ K (W m}^{-2}\text{)}^{-1}$ . The time constant characterizing the response of the upper ocean compartment of the climate system to perturbations is

---

S. E. Schwartz (✉)  
Atmospheric Sciences Division, Brookhaven National Laboratory, Upton, NY 11973, USA  
e-mail: ses@bnl.gov  
URL: <http://www.ecd.bnl.gov/steve>

estimated as about 5 years, in broad agreement with other recent estimates, and much shorter than the time constant for thermal equilibration of the deep ocean, about 500 years.

**Keywords** Climate sensitivity · Forcing · Global mean surface temperature · Heat capacity · Time constant

## 1 Introduction

Quantifying the response of Earth's climate system to radiative forcings, changes in the Earth radiation budget that are imposed externally to the climate system, is central to understanding prior climate change over the industrial period and to planning mitigation of and/or adaptation to future climate change. Imposition of a forcing, which induces an immediate imbalance in the top of the atmosphere (TOA) radiation budget, induces changes in the climate system, including change in global mean near-surface air temperature (GMST) and changes in the long- and short-wave components of the TOA radiation budget that would ultimately lead to restoration of the energy balance. A widely employed measure of climate system response to imposed perturbations is the so-called equilibrium climate sensitivity, conventionally defined as the long-term steady-state change GMST that would result from a sustained externally imposed change in global net absorbed radiation (forcing), normalized to this forcing.<sup>1</sup> Numerous climate model studies have indicated that such a change in GMST would be proportional to the magnitude of the imposed forcing, but relatively insensitive to nature of the forcing, and thus that the equilibrium sensitivity is an intrinsic property of Earth's climate system. Such studies indicate as well that other changes in climate scale with changes in GMST. Consequently, the equilibrium sensitivity is widely viewed as essential to assessing the magnitude of climate change, generally, that would result from a given forcing. Determining the equilibrium sensitivity has thus been the objective of much of the research endeavor directed to understanding Earth's climate and its response to perturbations.

Frequently, the equilibrium climate sensitivity is expressed as a "CO<sub>2</sub> doubling temperature"  $\Delta T_{2\times}$ , the amount by which GMST would ultimately increase in response to a sustained doubling of atmospheric CO<sub>2</sub>.  $\Delta T_{2\times}$  is related to the equilibrium sensitivity  $S_{eq}$  by  $\Delta T_{2\times} = F_{2\times} S_{eq}$ , where  $F_{2\times}$  is the forcing that would result from a doubling of CO<sub>2</sub>. The equilibrium sensitivity (or equivalently  $\Delta T_{2\times}$ ) is quite uncertain; the best estimate for  $\Delta T_{2\times}$  given by the 2007 assessment report of the Intergovernmental Panel on Climate Change (IPCC 2007) is 3 K, with an uncertainty range (central 66% of the probability distribution function) of 2–4.5 K (relative range 83%). This uncertainty greatly limits confidence in the interpretation of climate change over the industrial period and precludes effective planning of energy futures (Schwartz et al. 2010).

Broadly speaking, approaches to determining the climate sensitivity can be distinguished as model-based and observation-based. Model-based determination is generally taken to mean through the use of general circulation models (GCMs) of the Earth climate system. Such models are capable of imposing a forcing of known magnitude on the climate system

<sup>1</sup> For reasons having to do with stratospheric adjustment that occurs rapidly (months) following an increase CO<sub>2</sub>, which has traditionally been used as a benchmark forcing in model studies of climate sensitivity, the forcing pertinent to climate change and to determination of climate sensitivity has long been considered to be the change in net absorbed radiation at the tropopause. Increasingly, however, it is becoming recognized (e.g., Gregory and Forster 2008) that the measure of forcing pertinent to the global energy balance is the change in net radiation at the top of the atmosphere, again following such rapid adjustment.

and determining the sensitivity from the climate system response, accounting for the departure of the system from equilibrium through the net heating rate of the planet (Forster and Taylor 2006). Observationally based determination generally requires knowledge of both the forcing that is thought to have induced a change in GMST over a given period of time and the resultant temperature change attributable to that forcing, necessitating confident attribution of the response to the forcing. In principle, this approach might be based on equilibrium change in radiation and GMST over a long period of time, up to and including differences between glacial ice ages or the mid-Cretaceous and the present temperate period. Alternatively, the empirical approach might be based on shorter-term forcing and response, e.g., volcanic aerosols, or over the industrial period with time-dependent forcing, with some means of accounting for the observed response being only a fraction of the equilibrium response (Gregory et al. 2002; Forster and Gregory 2006; Murphy et al. 2009).

An intrinsic concern with determining the equilibrium climate sensitivity from long-time climate response to a perturbation is the long time required to approach a new steady state following imposition of a forcing, in the real world or in coupled atmosphere–ocean climate models, of the order of 1,000 years (Held et al. 2010; Hansen et al. 2011; Jarvis and Li 2011). Such a long response time makes it impractical to determine the equilibrium sensitivity by this long-time response, empirically or in climate models. The long time required to reach a new “equilibrium” also raises the question of the utility of the equilibrium sensitivity to societal decision-making about reducing carbon dioxide emissions to limit near-term global warming (Allen and Frame 2007).

Several investigators (Gregory 2000; Gregory and Forster 2008; Baker and Roe 2009; Held et al. 2010) have examined the response of Earth’s climate system to perturbations using two-compartment models that exhibit a rapidly achieved (decadal) near–steady-state response to a perturbation by a fast-responding compartment, which comprises the atmosphere, surface, and upper ocean and a much more slowly responding (multiple centuries) deep ocean compartment that is responsible for the slow approach to the ultimate steady state following imposition of a sustained forcing. In such models, in response to a (positive) forcing, there results, in addition to changes in the net irradiance at the top of the atmosphere (TOA), a flow of heat energy from the fast-responding compartment to the deep ocean, which has large heat capacity and long response time, that diminishes climate system response relative to the long-time response, in which the imposed forcing is offset only by change in net TOA irradiance. If the heat capacity and time constant of the deep ocean compartment are large compared to the upper compartment, the flow of heat energy into this compartment would be expected to be proportional to the change in global mean temperature. This situation leads in turn to an expected proportionality between the increase in GMST and imposed forcing that is achieved on decadal time scales. This proportionality is denoted here and elsewhere (Held et al. 2010; Padilla et al. 2011) as the *transient climate sensitivity*, although other terminology, e.g., “transient climate response,” (Dufresne and Bony 2008) is used.

Here, in order to determine the dependence of transient and equilibrium sensitivities on assumed forcing over twentieth century, I examine relations among observed changes in GMST, ocean heat content, and ocean heating rate, together with several published model-based estimates of forcing, all as a function of time. Interpretation of these relations within the two-compartment model yields quantities pertinent to climate system response to perturbations: the effective heat capacity of the climate system pertinent to climate change over this period, the heat uptake coefficient relating the rate of increase of planetary heat content and the increase in GMST, the coefficient of proportionality between increase in GMST and forcing (transient climate sensitivity), and the equilibrium climate sensitivity.

Estimates are also provided of the time constants for response of the two compartments to perturbations. Within the two-compartment model, all of these quantities are intrinsic properties of Earth's climate system. The effective heat capacity and heat uptake coefficient adduced by the present analysis are independent of assumptions about radiative forcing over this period, but the sensitivities are rather strongly dependent on the radiative forcing employed in the analysis.

The outline of this paper is as follows. Section 2 sets out the two-compartment model. Section 3 examines relations among the observables (GMST anomaly, ocean heat content anomaly, and global heating rate) and model-based estimates of global mean forcing and presents results for the climate system properties determined by this analysis. Section 4 places the findings in context with other work and examines concerns with the present analysis. Summary and conclusions are given in Sect. 5.

## 2 Theory

The energy conservation equation for Earth's climate system is

$$\frac{dH}{dt} \equiv N = Q - E \quad (1)$$

Here,  $H$  is the global heat content anomaly (relative to an arbitrary year or period);  $N \equiv dH/dt$  is the net heat flux into the planet;  $Q$  is the absorbed solar energy; and  $E$  is the emitted long-wave flux. Other sources or sinks of energy are negligible (Schwartz 2008b; Pilewskie 2011). In considering the consequences of a forcing, i.e., a radiative flux perturbation imposed on the climate system, it is useful to consider a situation in which a forcing is imposed on a system that is initially at radiative steady state (commonly denoted "equilibrium") in which the net flux is equal to zero:  $N_0 = 0$ . Whether such a situation is ever achieved is perhaps a question of threshold and averaging time. For example, fluctuations in the solar constant on an 11-year cycle would set a floor on the steadiness of the initial state; similarly, there are inevitably fluctuations arising from internal variability such as ENSO and from occasional forcing by aerosols from eruptive volcanos. In this steady-state situation, the emitted long-wave radiation, averaged over the planet and over a sufficiently long time (greater than a year, to average over seasonal variation), is very closely equal to the absorbed solar radiation:  $E_0 = Q_0$ .

Upon application of a perturbation in radiative flux, or forcing external to the climate system,  $F$ , the net flux into the climate system,  $N$ , is altered, a positive forcing corresponding to an increase in heat content of the system (positive  $N$ ),

$$N(t) = F(t) + Q(t) - E(t), \quad (2)$$

and the system responds by an increase in GMST; this increase in temperature and other changes in the climate system induced by the forcing result in changes in the absorbed and/or emitted power at the TOA. These changes are represented by an expression that denotes the dependence on GMST as a leading term but allows for dependence on higher order terms as well:

$$N = F + Q_0 - E_0 + \frac{\partial(Q - E)}{\partial T} \Delta T + \text{higher order terms}, \quad (3)$$

where the partial derivative denotes the changes in  $Q$  and  $E$  due to the response of the climate system to the change in temperature (but explicitly not including the change in net

flux that is the forcing itself). The first-order term would include changes in the climate system that scale with change in GMST, for example, surface long-wave irradiance, water vapor amount, and cloud amount. The higher order terms would include terms that are second order in  $\Delta T$  and any dependence on geographical or temporal distribution of change in surface temperature. As is conventional, the effects of these higher order terms are omitted in the analysis that leads to a climate sensitivity. In the present analysis, I restrict consideration to the first-order term, but I return to consideration of the higher order terms and their implications in Sect. 4.5.

Conventionally, the partial derivative in Eq. 3 is expressed as a *climate response coefficient*,

$$\lambda \equiv -\frac{\partial(Q-E)}{\partial T}, \quad (4)$$

the sign of which is chosen to make  $\lambda$  a positive quantity. For a positive forcing, initially  $N$  is increased by the magnitude of the forcing; as the temperature increases in response to this forcing, the value of  $N$  decreases as the system approaches a new steady state. For this constant forcing,  $N$  again approaches zero, and, under the assumption that the properties of the climate system affecting the climate system response to the forcing are unchanged as the new equilibrium is reached,  $\Delta T$  would be equal to  $\lambda^{-1}F$ . The inverse of  $\lambda$ ,  $S_{\text{eq}} \equiv \lambda^{-1}$  is denoted the *equilibrium climate sensitivity*, the amount by which GMST would ultimately change in response to a sustained forcing, normalized to the value of the forcing, for properties of the climate system affecting the partial derivative in Eq. 4 unchanged. By this definition,

$$S_{\text{eq}} = \lambda^{-1} = \left[ \left( \frac{\partial(Q-E)}{\partial T} \right)_0 \right]^{-1},$$

where the subscript 0 denotes a given unperturbed climate state, the equilibrium sensitivity is seen to be a property of Earth's climate system and thus of intrinsic, as well as practical, interest.

Commonly, especially in the context of examining the consequences of alternative scenarios of future CO<sub>2</sub> emissions, the equilibrium sensitivity is expressed as the amount by which the global mean surface temperature would ultimately increase in response to a sustained doubling of atmospheric CO<sub>2</sub>, CO<sub>2</sub> *doubling temperature*,  $\Delta T_{2\times}$ ; within the linear range of the relation between increase in GMST and forcing,  $\Delta T_{2\times}$  is equal to  $F_{2\times}S_{\text{eq}}$ , where  $F_{2\times}$  is the forcing corresponding to a doubling of CO<sub>2</sub>, which is about 3–4 W m<sup>-2</sup>.  $F_{2\times}$  is commonly (Myhre et al. 1998; IPCC 2007) given, or readily inferable, as 3.71 W m<sup>-2</sup>, although that precision is hardly justified by the accuracy with which  $F_{2\times}$  is known for the actual climate system (Stevens and Schwartz 2012) or represented in current climate models (Webb et al. 2006; Forster and Taylor 2006) because, *inter alia*, of issues involving radiation transfer, especially in cloudy atmospheres (Collins et al. 2006), and short-term responses of clouds to changes in CO<sub>2</sub> (Andrews et al. 2009). In this paper, the primary results for climate sensitivity are presented in systematic units, K (W m<sup>-2</sup>)<sup>-1</sup>, with values of  $\Delta T_{2\times}$ , evaluated with  $F_{2\times}$  taken as 3.71 W m<sup>-2</sup>, presented for convenience.

Equation 3 (*cf.* also, Gregory and Forster 2008) suggests a direct proportionality (constant ratio) between  $\Delta T(t)$  and  $F(t)-N(t)$ , where the dependence of all quantities on secular time  $t$ , as would result from temporally variable forcing, is explicitly noted,

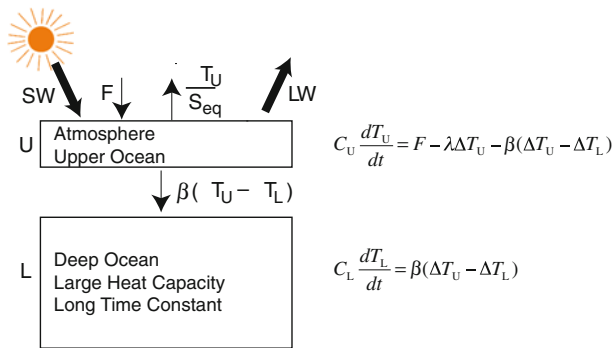


**Fig. 1** Two-compartment model for Earth’s climate system, consisting of *upper* compartment U with small heat capacity  $C_U$  and short time constant for reaching steady state following a perturbation, and *lower* compartment L with large heat capacity  $C_L$  and long time constant for reaching steady state. *Thick arrows* denote initial short-wave (SW) and long-wave (LW) fluxes, and *thin arrows* denote perturbations: forcing  $F$  and resultant heat flows, a change in net top-of-atmosphere irradiance given by the time-dependent forcing minus the time-dependent change in temperature  $\Delta T_U$  of the *upper* compartment upon the equilibrium sensitivity  $S_{eq}$ , and a heat flux from the *upper* compartment to the *lower* compartment L given by the heat exchange coefficient  $\beta$  times the difference in temperature changes between the *upper* ( $\Delta T_U$ ) and *lower* ( $\Delta T_L$ ) compartments

$$F(t) - N(t) = \lambda \Delta T(t), \quad (5)$$

or, equivalently, in terms of the equilibrium sensitivity

$$\Delta T(t) = S_{eq}(F(t) - N(t)). \quad (6)$$

Equation 6 leads to the hypothesis that a plot of  $\Delta T(t)$  versus  $F(t) - N(t)$ , for both  $F(t)$  and  $\Delta T(t)$  measured from the same initial steady-state condition, would be expected to be linear through the origin with slope  $S_{eq}$  and thus that  $S_{eq}$  can be determined as the slope. To distinguish this method of determining  $S_{eq}$  from a second method described below, I denote this approach to determining the equilibrium sensitivity the “ $F$ – $N$  method”.

A second approach to determining climate sensitivity is based a simple two-compartment model of the climate system illustrated in Fig. 1 (*cf.* also Gregory 2000; Held et al. 2010). The upper compartment, which consists principally of the atmosphere and the upper ocean, is coupled radiatively to the incoming solar irradiance and the outgoing thermal infrared radiation at the TOA and thermally to the deep ocean compartment. A positive forcing applied to the climate system induces an increase in the temperature of the upper compartment that induces not only a radiative response identical to that described above (Eq. 3) but also a heat flow into the larger-heat-capacity deep-ocean compartment. It is posited that the time required for the lower compartment to respond to any forcing is much greater than that for the upper compartment; Held et al. (2010) refer to this compartment as “recalcitrant” to changes in heat content. For an initial estimate of the heat capacities of the upper compartment from the depth of the mixed layer (ca., 100 m) and of the lower compartment from the average depth of the world ocean (ca 3,800 m), the ratio of the heat capacities would be approximately 40. Hence, following imposition of an external forcing, it would be expected that the temperature change of the lower compartment would be much less than that of the low-heat-capacity, rapidly accommodating upper compartment. This leads to the hypothesis that the rate of heat transport from the upper compartment to

the lower compartment would be proportional to the increase in temperature of the upper compartment  $\Delta T$ ; cf. also Forster and Taylor (2006), Boer et al. (2007), Gregory and Forster (2008). Observationally, as shown below, the rate of increase of heat content of the climate system is found to be proportional to  $\Delta T$ ,

$$N(t) = \kappa \Delta T(t). \quad (7)$$

The *heat uptake coefficient*  $\kappa$ , like the equilibrium climate sensitivity, is posited to be an intrinsic property of Earth's climate system.

The two-compartment model (Gregory 2000; Knutti et al. 2008, Schwartz 2008a; Held et al. 2010) exhibits two time constants (inverses of the eigenvalues) that characterize the rate of relaxation of the system to a perturbation. Specializing to the situation in which the lower compartment is much larger than the upper compartment, and has much greater heat capacity  $C_L$  than that of the upper compartment  $C_U$ , yields (Held et al. 2010) for the two time constants (to first order in  $C_U/C_L$ )

$$\tau_s = \frac{C_U}{\beta + \lambda} \quad \tau_l = C_L \left( \frac{1}{\lambda} + \frac{1}{\beta} \right), \quad (8)$$

where the subscripts *s* and *l* denote short and long time constants characterizing the response of the upper and lower compartments, respectively. Although it does not appear that these time constants can be exactly determined by the present analysis, as shown below, they can be estimated based on observations and reasonable assumptions.

The two-compartment model suggests that the heat capacities of the two compartments of the climate system may be identified as follows. The heat capacity of the large compartment is that of the global ocean, which may be evaluated as the volume of the global ocean times the volumetric heat capacity seawater. For the fractional area of Earth covered by ocean as 0.71 and the average depth of the world ocean taken as 3,800 m, the average depth per area of the entire planet is 2,700 m. For the volumetric heat capacity of seawater taken as  $4.0 \times 10^6 \text{ J m}^{-3} \text{ K}^{-1}$ , the areal heat capacity (per area of the planet)  $C_L = 1.1 \times 10^{10} \text{ J m}^{-2} \text{ K}^{-1}$ . For climate change considerations, it is convenient to express this heat capacity in the unit  $\text{W year m}^{-2} \text{ K}^{-1}$ , yielding  $C_L = 340 \text{ W year m}^{-2} \text{ K}^{-1}$ . An effective heat capacity of that part of the climate system that is coupled to the change in global temperature may be obtained (Schwartz 2007) from the relation between the observed change in global heat content  $H$  and the observed change in GMST. As shown previously (Schwartz 2007) and updated below for the further available measurements, a linear relation is obtained between ocean heat content anomaly and global temperature anomaly,

$$H_{\text{ocn}} = H_0 + C_{\text{ocn}} \Delta T, \quad (9)$$

allowing an effective ocean heat capacity to be evaluated as the slope of a graph of the two quantities. The heat capacity thus determined is then augmented to account for other heat sinks (heating of the atmosphere and upper solid earth; melting of ice) to yield an estimate for the effective heat capacity of the climate system,  $C_{\text{eff}}$ . As determined below, this quantity is more than an order of magnitude less than  $C_L$ , consistent with the two-compartment model outlined above and with the expressions for the time constants given in Eq. 8.

A proportionality between global heating rate and the increase in GMST would result in a further proportionality, between the time-dependent increase in GMST  $\Delta T(t)$  and the time-dependent forcing  $F(t)$ : from Eqs. 5 and 7,

$$F(t) = (\kappa + \lambda)\Delta T(t). \quad (10)$$

Equation 10 suggests a so-called *transient climate sensitivity* analogous to the equilibrium sensitivity,

$$S_{tr} \equiv (\kappa + \lambda)^{-1} \quad (11)$$

that relates the time-dependent increase in surface temperature to the time-dependent forcing,

$$\Delta T(t) = S_{tr}F(t), \quad (12)$$

which implies that a graph of  $\Delta T(t)$  versus  $F(t)$  would be linear through the origin, with slope  $S_{tr}$ . This transient climate sensitivity is the same quantity as that determined from observed temperature change and modeled forcing by Gregory and Forster (2008), except that their quantity is referred to the forcing of doubled  $\text{CO}_2$  and is thus greater by a factor of 3.7.

The temperature response to a step-function forcing of the two-compartment system with a given transient sensitivity and upper compartment time constant is initially virtually identical to that of a single compartment system having the same time constant and equilibrium sensitivity, Fig. 2a; the influence of the long-time-constant, large-heat-capacity, lower compartment initially is to provide a further heat sink, in addition to the decrease in net radiation absorbed at the TOA (Eq. 3), that diminishes the initial temperature response. Only at long times, appreciable relative to the time constant of the lower compartment, when the increase in temperature of the lower compartment  $\Delta T_L$  becomes appreciable relative to the increase in temperature of the upper compartment  $\Delta T_U$  (Fig. 1), does the heat transport to the lower compartment become appreciably reduced, and the temperature of the upper compartment approaches its “equilibrium” value, Fig. 2b. The plateau in the temperature change of the upper compartment shown in Fig. 2a is the basis of the transient sensitivity concept.

In order to determine the transient and equilibrium sensitivities and their dependence on assumed forcing over twentieth century, the present study examines the several proportionalities between observations of temperature change, planetary heat content, and heating rate over the twentieth century,  $\Delta T(t)$ ,  $\Delta H(t)$ , and  $N(t)$ , and between these observables and estimates of the forcing over this period,  $F(t)$ , as follows:  $H(t)$  versus  $\Delta T(t)$ , slope,  $C_{\text{eff}}$ .

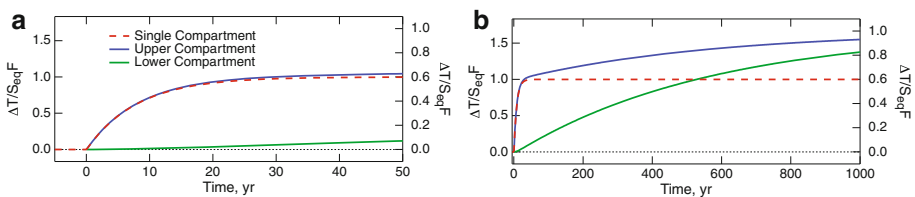


**Fig. 2** Normalized temperature response of one- (*left axis*) and two-compartment (*right axis*) models to step-function forcing initiated at time = 0. Equilibrium sensitivity of one-compartment model and transient sensitivity of two-compartment model are  $0.4 \text{ K (W m}^{-2}\text{)}^{-1}$  ( $\Delta T_{2\times} = 1.5 \text{ K}$ ); equilibrium sensitivity of two-compartment model is  $0.67 \text{ K (W m}^{-2}\text{)}^{-1}$  ( $\Delta T_{2\times} = 2.5 \text{ K}$ ). Heat exchange coefficient in two-compartment model is  $1 \text{ W m}^{-2} \text{ K}^{-1}$ . Time constant of one-compartment model and of *upper* compartment of two-compartment model is 8 years; time constant of *lower* compartment is 570 years. Heat capacity of upper compartment and *lower* compartment are 20 and  $340 \text{ W year m}^{-2} \text{ K}^{-1}$ , respectively. *Vertical axes* are scaled by the ratio of the equilibrium sensitivities of the two models



(Eq. 9);  $N(t)$  versus  $\Delta T(t)$ , slope  $\kappa$ , Eq. 7;  $\Delta T(t)$  versus  $F(t)$ , slope  $S_{tr}$ , Eq. 12;  $\Delta T(t)$  versus  $F(t) - N(t)$ , slope  $S_{eq}$ , Eq. 6. Note that (except for the relation between  $H$  and  $\Delta T$ ) each of these several relations is a *proportionality*, that is, a linear relation with zero intercept. The order of the relation indicates the dependent and independent variables, respectively, under the expectation that the temperature change depends on the forcing but that the heat content and heating rate depend on the temperature change. The relation between  $S_{eq}$  and  $S_{tr}$ ,

$$S_{eq} = \frac{1}{S_{tr}^{-1} - \kappa}, \quad (13)$$

leads to a second method of estimating of  $S_{eq}$  based on the heat uptake coefficient  $\kappa$  rather than the individual measurements of heating rate  $N(t)$ ; I denote this method the “ $\kappa$  method”.

The estimates of climate sensitivities obtained in this way are not wholly observationally based but are hybrids between observationally and model-based estimates of these quantities, as the time-dependent forcing is not directly observed but is based on radiative transfer calculations for measured or modeled changes in atmospheric composition. Examining these quantities for a suite of forcing estimates allows assessing the consistency of the model and the estimates of forcing, which would be manifested by a linear proportionality of temperature change and forcing, and determination of the dependence of the inferred climate sensitivities on the forcing.

This entire analysis is rooted in the forcing-response model of climate change, that is, that the change in global mean temperature is a consequence only of forcing under the assumption that forcings are fungible and that GMST response, normalized to forcing, is independent of the nature and geographical distribution of the forcing. I return to this point in Sect. 4.5.

### 3 Results and Interpretation

#### 3.1 Global Heat Content and Heating Rate

The major accessible reservoir for storing planetary heat energy is the world ocean on account of the high specific heat of water and the relatively rapid rate of heat exchange within the ocean by virtue of circulations and turbulent mixing on a variety of scales. The basis for determination of the global heating rate rests on the data base of historical measurements of ocean temperature as a function of location, depth, and time. These temperature measurements are converted into heat content anomaly as a function of time (relative to a specified base period) via the heat capacity of ocean water and integration over the volume of the world ocean. The measurement data base extends back to about 1950, but the early measurements are sparse, and there remain questions about the accuracy of the primary measurements and the coherence of measurements by different types of sounding instruments and platforms, which have changed over time (Gouretski and Reseghetti 2010). The measurements have been analyzed by several groups, with broad agreement but significant differences based on differences of approach and assumptions about measurement techniques; for reviews, see Palmer et al. (2010) and Lyman (2011). A composite of the data compilations for anomaly of heat content of the world ocean from the surface to 700 m is shown in Fig. 3; most of the increase in ocean heat content is due to

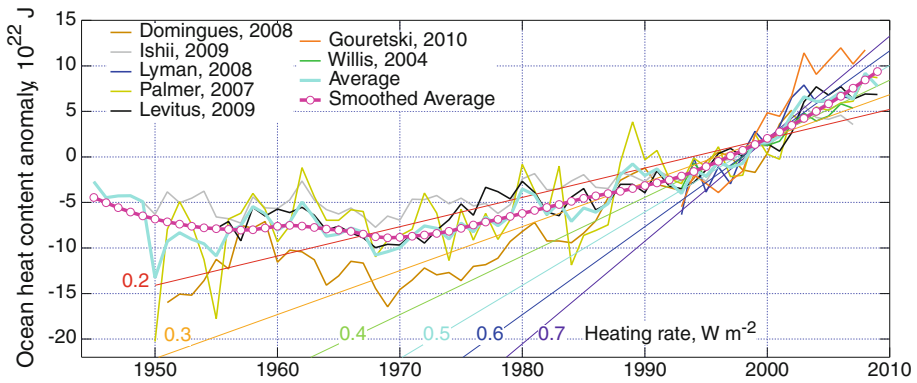


**Fig. 3** Recent evaluations of ocean heat content anomaly (0–700 m), relative to 1993–2002. Also shown are the average of the several estimates and a LOWESS smoothed curve based on the average. Slopes of lines show heating rate referred to Earth surface area. Data from <http://www.ncdc.noaa.gov/bams-state-of-the-climate/2009-time-series/ohc> (retrieved November 5, 2010) which gives the citations to the publications; data have been updated from the indicated publications by Palmer et al. (2010)

warming within the top 700 m, and most of that within the top 300 m (Levitus et al. 2005). Also shown in the figure is the average of the data obtained by the several groups; in order not to bias the average at times where different data sets contributed to the average, all anomalies were computed relative to the years 1993–2002, for which period all data sets are represented.

The effective areal heat capacity of the portion of the climate system that is actively coupled to the change in global temperature  $C_{\text{eff}}$  is evaluated from the dependence of the change in ocean heat content on the change in global temperature. As seen in Fig. 4, a linear relation is exhibited between the areal heat content anomaly of the ocean (to 700 m) and the surface temperature anomaly; the fit was restricted to the data subsequent to 1965, consistent with the analysis for heating rate, but the slope for the entire data set (subsequent to 1945) differed negligibly. The slope of this plot,  $14.1 \pm 1.0 \text{ W year m}^{-2} \text{ K}^{-1}$ , represents an effective areal heat capacity of the upper 700 m of the world ocean. This effective heat capacity is well less the actual areal heat capacity of seawater to this depth, evaluated as the fractional area of the world ocean, 0.71, times the volumetric heat capacity of seawater,  $4.0 \times 10^6 \text{ J m}^{-3} \text{ K}^{-1}$ , times the depth, 700 m, and expressed in the same units,  $63 \text{ W year m}^{-2} \text{ K}^{-1}$ , indicative of the fact that the entire global amount of seawater to this depth is not in thermal equilibrium with the increasing global temperature but is substantially lagging the increase in temperature. Accounting for heating of the ocean deeper than 700 m adds another 30% to this effective heat capacity, yielding  $18.3 \text{ W year m}^{-2} \text{ K}^{-1}$ . An alternative way of looking at this result is that this heat capacity corresponds to a hypothetical depth of seawater in thermal equilibrium with the surface temperature, 145 m (for the entire planet) or 200 m for ocean fractional area of 0.71. Finally, accounting for heat sinks in the climate system (air, solid earth, melting of ice) adds a further 19% to the effective heat capacity, yielding  $21.8 \pm 2.1 \text{ W year m}^{-2} \text{ K}^{-1}$ , where the uncertainty is a one-sigma estimate that takes into account the uncertainty in the slope together with estimated uncertainties (25%) in the two augmentations.

Determining the heating rate of the global ocean requires taking a derivative of the heat content; this is complicated by the temporal variability of the data. This variability may be noise associated with the measurements and/or may be a manifestation of actual variability

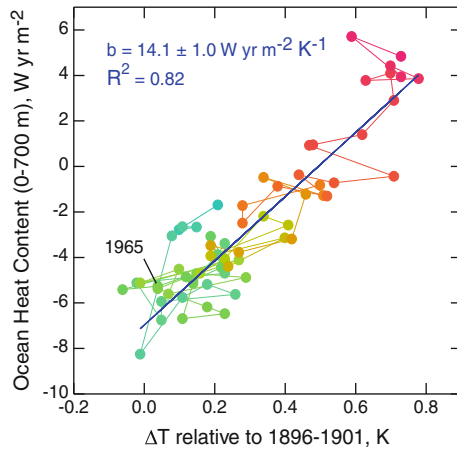


**Fig. 4** Examination of relation between global ocean heat content anomaly and temperature anomaly (Eq. 9). Heat content anomaly of the world ocean, relative to 1993–2002, from surface to 700 m, expressed per area of the planet (Fig. 3) is plotted against global mean surface temperature anomaly relative to 1896–1901  $\Delta T_{1900}$ . Fit to data in the form  $\Delta H = a + b\Delta T$  (Eq. 9) is evaluated for data from 1965 through 2009; uncertainty in regression slope is standard error, neglecting autocorrelation. Also indicated as  $R^2$  is fraction of variance in the original data accounted for by the regression. Colors of data points denote date, from 1945 (light blue) to 2009 (red)

of ocean heat content, a consequence perhaps of internal climate variability such as ENSO or of change in heating rate due to variability in forcing, such as by volcanic aerosol forcing. In order to smooth the data to permit taking the time derivative, the LOWESS algorithm (locally weighted scatterplot smoothing; Cleveland and Devlin 1988) was used to construct a smooth curve that retained the slow temporal variability of the data (magenta curve in Fig. 3); the areal heating rate of the ocean was obtained as the derivative of this quantity. A sense of the magnitude of the slope is provided by auxiliary lines drawn on the figure whose slopes correspond to the heating rates indicated, in units of watts per square meter, expressed relative to the total Earth surface area ( $5.1 \times 10^{14} \text{ m}^2$ ), not just the area of the world ocean. There is indication that since 1970, the slope has been increasing from perhaps  $0.3 \text{ W m}^{-2}$  to perhaps  $0.6 \text{ W m}^{-2}$ .

Accounting for additional ocean heat uptake and other heat sinks, as with ocean heat content, yields the rate of global heating shown as a function of time in Fig. 5. Prior to about 1970, the heating rate exhibited fairly large fluctuations and indication even of negative values (net cooling of the planet); these fluctuations may be due to sampling or measurement issues or may reflect actual changes in global heat content. Subsequent to about 1970, the rate of change of global heat content has been consistently positive, albeit not monotonically increasing until after about 1992. Although this variable pattern may again be a consequence of sampling or measurement issues, that possibility seems increasingly unlikely in the later time frame on account of the increase in number and quality of the data and the general tightness of the several compilations of the ocean heat content data. In further support of this argument is the general agreement of the increase in heating rate  $N$  with the increase in GMST over the entire time period from about 1960 to the present shown in the time series in Fig. 5.

The relation between global heating rate and global mean surface temperature anomaly (Eq. 7) is examined further in Fig. 6, in which the heating rate is plotted against global temperature anomaly relative to 1900,  $\Delta T_{1900}$ . For the fit restricted to the data from 1965 to

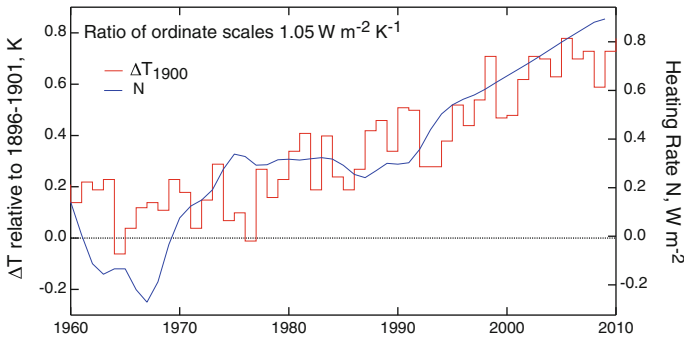


**Fig. 5** Global mean surface temperature anomaly relative to 1896–1901  $\Delta T_{1900}$  (left axis), evaluated from the Goddard Institute for Space Studies (GISS) Combined Land–Surface Air and Sea–Surface Water Temperature Anomalies (Land–Ocean Temperature Index, LOTI) <http://data.giss.nasa.gov/gistemp/tabledata/GLB.Ts+dSST.txt>, (Hansen et al. 2010) and global heating rate  $N$  (right axis) evaluated as derivative of smoothed average ocean heat content anomaly shown in Fig. 3, augmented to account for deep ocean heating and other heat sinks as described in text, and expressed per area of the planet. Ordinate axes are scaled by the slope of regression forced through the origin (Fig. 6)

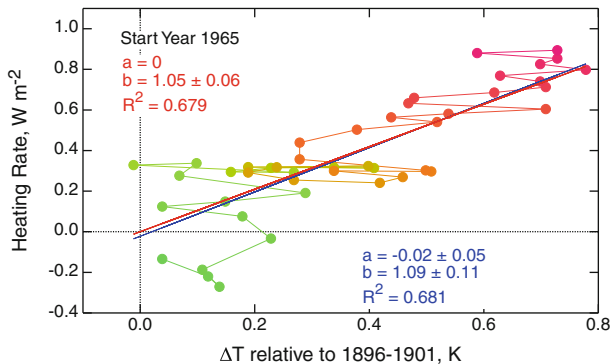


**Fig. 6** Examination of proportionality between global heating rate and temperature anomaly (Eq. 7). Global heating rate (evaluated as derivative of smoothed average ocean heat content anomaly shown in Fig. 3, augmented to account for deep ocean heating and other heat sinks as described in text and expressed per area of planet) is plotted against global mean surface temperature anomaly relative to 1896–1901  $\Delta T_{1900}$ . Fits to data in the form  $dH/dt = a + b\Delta T$  are evaluated for data from 1965 through 2009, with and without constraining regression line to pass through origin; uncertainties in regression coefficients are standard error, calculated under assumption of no autocorrelation. Also indicated as  $R^2$  is fraction of variance in the original data accounted for by the regression. Colors of data points denote date from 1965 (green) to 2009 (red)

the present, the regression line has an intercept quite close to zero,  $-0.02 \pm 0.05 \text{ W m}^{-2}$  (1 sigma, calculated under assumption of zero autocorrelation), and the regression fit constrained to pass through the origin accounts for virtually the same fraction of the variance (68%) as the two parameter fit, that is, the heating rate is proportional to the increase in surface temperature relative to 1896–1901. This finding is relatively insensitive to the start date of the correlation, with intercept ranging from  $-0.06 \pm 0.05 \text{ W m}^{-2}$  (start date 1960) to  $+0.10 \pm 0.04 \text{ W m}^{-2}$  (start date 1970), so the finding of linear proportionality (zero intercept) would appear to be robust. The corresponding values for the slope of the regression forced through the origin are  $1.02 \pm 0.06$ ,  $1.05 \pm 0.06$ , and  $1.07 \pm 0.05 \text{ W m}^{-2} \text{ K}^{-1}$  for start date 1960, 1965, and 1970, respectively. The rather tight

correlation between global heating rate (as inferred from ocean heating rate) and the increase in global temperature relative to the beginning of the twentieth century supports the hypothesis that this heating rate is proportional to global mean surface temperature anomaly, Eq. 7, with heat uptake coefficient  $\kappa = 1.05 \pm 0.06 \text{ W m}^{-2} \text{ K}^{-1}$ . The proportionality of heating rate and global temperature, independently determined, is consistent with the two-compartment model with a much greater heat capacity in the lower compartment, as described above and supports the utility of using the time-dependent heating rate and/or the regression slope in examination of the relation between global temperature change and various estimates of forcing over the twentieth century.

### 3.2 Forcing

The observationally based determination of climate sensitivity rests on knowledge of climate forcing over the instrumental record. Knowledge of this time-dependent forcing is required also in climate model calculations over the twentieth century. Two approaches have been taken in climate modeling studies to determine the forcing. The forcing may be specified as an input to the model based on measured or modeled changes in atmospheric composition and other radiation influencing quantities. Alternatively, the atmospheric substances influencing radiation in the model are themselves modeled within the climate model, and the resulting changes in radiation are calculated within the climate model. The latter approach is increasingly being taken by various modeling groups (Lohmann et al. 2010). As a consequence, it seems to be difficult to extract the forcing from climate model runs of the twentieth century. An examination of the literature revealed only a limited number of forcing data sets that were suitable for the present study. In addition to anthropogenic gases and aerosols, whose forcings are to be calculated, modeling the twentieth century requires representation of natural forcings by changes in solar irradiance and, importantly, forcing by stratospheric aerosols that result from eruptive volcanoes. Volcanic eruptions in the twentieth century have resulted in several instances of short-duration forcing, the magnitudes of which are substantial in the context of anthropogenic forcing, and which are manifested in the record of GMST. The several explicitly calculated time series of forcing over the twentieth century available from the literature are summarized in Table 1. In addition to the data sets examined here, Forster and Taylor (2006) have presented forcing data sets inferred from the increase in GMST in AR4 model runs over the twentieth century together with the transient sensitivity of these models determined from model runs with 1% per year increment  $\text{CO}_2$ , for which the forcing is known. The approach appears to yield a fairly accurate estimate of the time-dependent forcing as shown by comparison with forcing data sets employed in the GISS (Goddard Institute for Space Studies; Hansen et al. 2005) and MIROC (Model for Interdisciplinary Research On Climate; Takemura et al. 2006) model studies for which forcings were explicitly calculated. This method was subsequently applied to determine the forcing time series over the twentieth century in the Hadley Centre model (Jones et al. 2011). In view of the indirect means of inferring the forcing, these forcing data sets were not examined in the present study, although doing so might provide further insight.

The forcing data set employed in climate model studies by the investigators at the Goddard Institute for Space Studies (GISS; Hansen et al. 2005), Fig. 7, is illustrative of current forcing data sets. The positive (warming) forcing by the well mixed greenhouse gases (GHGs) and the negative (cooling) forcings due to scattering and cloud-brightening effects of aerosols exhibit relatively smooth increases in magnitude with similar temporal trend. Negative forcing by volcanic stratospheric aerosols in contrast is highly irregular,

**Table 1** Forcing data sets examined in this study

Data Set	Reference and data source	Forcing, 1900–1990, $W\ m^{-2}$
PCM, parallel climate model, national center for atmospheric research	Meehl et al. (2003), Fig. 1; numerical file provided by G. Strand, 2011	2.1
GFDL, geophysical fluid dynamics laboratory	Held et al. (2010), Fig. 2; numerical file provided by I. Held, 2011	1.9
GISS, goddard institute for space studies	Hansen et al. (2005), Fig. 1a; <a href="http://data.giss.nasa.gov/modelforce/RadF.txt">http://data.giss.nasa.gov/modelforce/RadF.txt</a>	1.6
RCP—representative concentration pathways	Meinshausen et al. (2011); <a href="http://www.pik-potsdam.de/~mmalte/rcps/data/20THCENTURY_MIDYEAR_RADFORCING.xls">http://www.pik-potsdam.de/~mmalte/rcps/data/20THCENTURY_MIDYEAR_RADFORCING.xls</a>	1.6
MIROC, model for interdisciplinary research on climate	Takemura et al. (2006), Fig. 2a; numerical file provided by T. Takemura, 2011.	1.1
Myhre	Myhre et al. (2001), Fig. 1; <a href="http://folk.uio.no/gunnarmy/data/rf_time.dat">http://folk.uio.no/gunnarmy/data/rf_time.dat</a>	1.0

Column 3 gives forcing in 1990 (prior to the 1991 Pinatubo eruption) relative to the average for 1896–1901 (also relatively free of influences of volcanic aerosols) used to relate inferred climate properties to twentieth century forcing

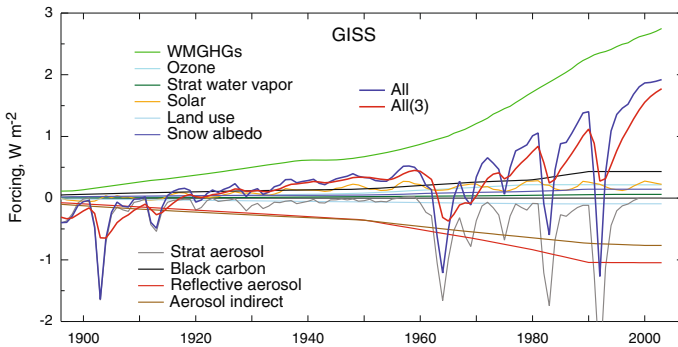


**Fig. 7** Global mean forcings (relative to 1880) as employed in the Goddard Institute for Space Studies (GISS) climate model (Hansen et al. 2005; <http://data.giss.nasa.gov/modelforce/RadF.txt>). WMGHGs, well mixed greenhouse gases. “All” denotes the total forcing, the sum of the individual forcings, and “All(3)” denotes that forcing convolved with the function  $\exp(-t/3) [1 - \exp(-1/3)]$

exhibiting large values immediately following volcanic eruptions, but decaying to near zero over the course of a few years. Other forcings are relatively small, even in the aggregate. Solar forcing exhibits a cyclical behavior with a roughly 11-year period, indicative of the change in the solar constant associated with the sunspot cycle. Forcings by black carbon from incomplete combustion offset part of the negative aerosol cooling forcing. There are minor contributions from the increase in tropospheric and stratospheric ozone, and the increase in stratospheric water vapor resulting from the increase in tropospheric methane, some of which makes its way into the stratosphere and is oxidized there. Changes in surface albedo from black carbon on snow and from land use changes also make minor contributions. The total forcing, evaluated as the sum of the several components, exhibits a general positive trend over the period but is punctuated by the large, short-duration negative forcings by volcanic stratospheric aerosols, such that the total forcing can, even in the latter part of the twentieth century, exhibit brief excursions into negative values (relative to 1880) before returning to the gradual positive forcing.

In order to relate forcing to temperature change, it is necessary to take into account the damping effect of global surface temperature on the rapid impulses in forcing associated with volcanic eruptions. The approach I have taken is to impose a damping on the forcing by convolving the total forcing from the several data sets with a decaying exponential function having a 3-year time constant,  $\exp(-t/3) [1 - \exp(-1/3)]$ , where  $t$  is time in years and  $[1 - \exp(-1/3)]$  is a normalization factor. As expected, this damped forcing, also shown in Fig. 7, exhibits reduced magnitude but extended duration of the stratospheric volcanic aerosol forcing. To assess the suitability of this approach, I compared the time series of the damped forcing with that of observed global mean surface temperature anomaly, Fig. 8. It is seen that the two time series exhibit qualitatively similar behavior in the response to the impulses due to volcanic aerosols, suggesting that the 3-year exponential function is doing a reasonable job of accounting for the time lag of global temperature to the volcanic forcing, especially during the latter half of the twentieth century during which the volcanic aerosol forcings are perhaps better characterized. The 3-year time constant is similar to that found in analysis of GCM data by Held et al. (2010),  $4 \pm 1$  years, but is somewhat shorter than that determined from analysis of autocorrelation of global mean temperature data, 6–11 years (Scafetta 2008; Schwartz 2008a). A fairly short damping time constant is desired so as to minimize any artificial lag of the more

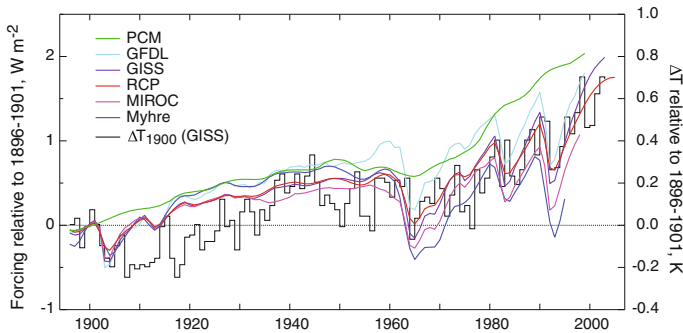


**Fig. 8** Total forcings from the several forcing data series examined in this study, convolved with the function  $\exp(-t/3) [1 - \exp(-1/3)]$ . Also shown for comparison is the time series of global mean surface temperature anomaly as tabulated by the Goddard Institute for Space Studies (GISS; Combined Land-Surface Air and Sea-Surface Water Temperature Anomalies, LOTI; <http://data.giss.nasa.gov/gistemp/tabledata/GLB.Ts+dSST.txt>)

slowly varying forcings arising from the gradual increases in greenhouse gases and aerosols.

Also shown in Fig. 8 are the time series for the several other forcing data sets examined in this study, similarly convolved with the 3-year exponential decay function. With the exception of the PCM data series, which did not include volcanic aerosol forcing, all the data series exhibit qualitatively similar behavior over the time period, and all exhibit an increase in forcing over the twentieth century, reflecting the dominant contribution of forcing by GHGs. However, closer comparison of the several data sets, Fig. 9, shows considerable differences among them. Examination of the scatter plots shows strong correlation of the GISS, RCP, GFDL, and MIROC forcings but with offsets from the diagonal, which would indicate perfect agreement. Not surprisingly, the PCM forcing data set exhibits poorer correlation because of volcanic aerosol forcing not being included in that data set; this is manifested by downward departure of the other data sets from the PCM data set in “streamers” associated with periods of volcanic aerosol forcing. The data set of Myhre et al. (2001) exhibits rather poor correlation with the other forcing data sets.

### 3.3 Correlation of Temperature Anomaly and Forcing

As the intent of this study is to examine the relation of the change in GMST to radiative forcing over the twentieth century, for which the forcing and temperature data are available, it was considered essential that the forcing and temperature anomaly time series be defined relative to values of these quantities in a common time period at the beginning of the century. As the variation in the several data sets over the base period 1896–1901 is quite small relative to variation over the data set as a whole (Fig. 8), the average over this time period was taken as the reference value for both forcing and temperature change.

Attention is called also to the large range of forcing over the full span of the time series. To some extent, this is a consequence of the differing end dates of the time series; it might be argued that the time series of Myhre et al., which terminates in 1995, is not fully recovered from the Pinatubo event. However, even so, in 1990, prior to the Pinatubo eruption, the forcing in the six data sets, Table 1, exhibits a span of a factor of 2 and a



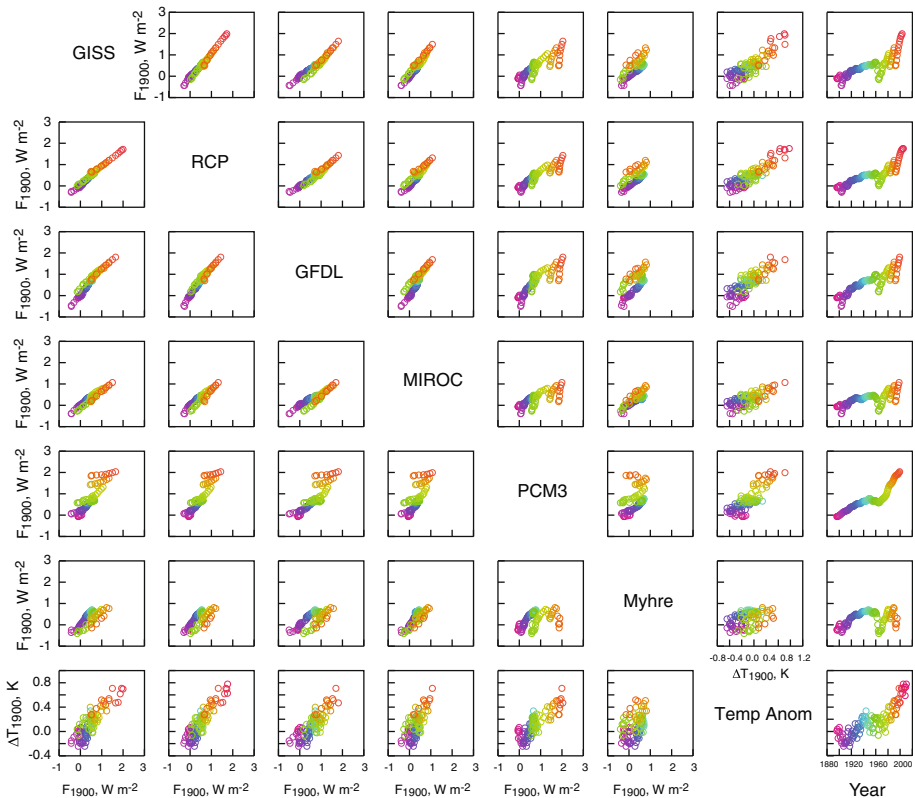


**Fig. 9** Scatterplot matrix of the several forcings (relative to 1896–1901) employed in this study and also global mean surface temperature anomaly (also relative to 1896–1901). The column and row headings of the several data sets are given along the trace of the matrix, and each graph represents a scatter plot of the quantity identified by the row heading on the y axis versus the quantity identified by the column heading on the x axis. All of the forcings are shown on the same scale; perfect agreement between two different forcing data sets would be manifested by all data lying along the diagonal. Similarly a linear dependence of temperature anomaly on forcing would be manifested by a linear array of the data points. The *right hand* column in the matrix of graphs gives the time series of each of the forcings and temperature anomaly. The *color coding* reflects the date (*violet*, 1896 to *red*, 2009)

relative range (range divided by median) of 69%. This range is characteristic of, but well less than, the uncertainty in total forcing over the twentieth century, as given in the IPCC Fourth Assessment Report (2007), best estimate  $1.6 W m^{-2}$ ; 90% confidence range ( $0.6\text{--}2.4 W m^{-2}$ ), or relative range 113%. A range in forcing will inevitably lead to a corresponding range in any assessment of climate sensitivity that is obtained using the several values of forcing together with the time series of observed surface temperature. A key objective of this study is to assess the range in transient and equilibrium sensitivities that results from the range of forcing estimates.

The relation between surface temperature anomaly and forcing was examined by means of graphs of surface temperature anomaly relative to the 1896–1901 base period versus forcing relative to the same period, Fig. 10; these graphs are the same as in the bottom row of Fig. 9. The y-data of all graphs are the observed temperature change; the x-data, the

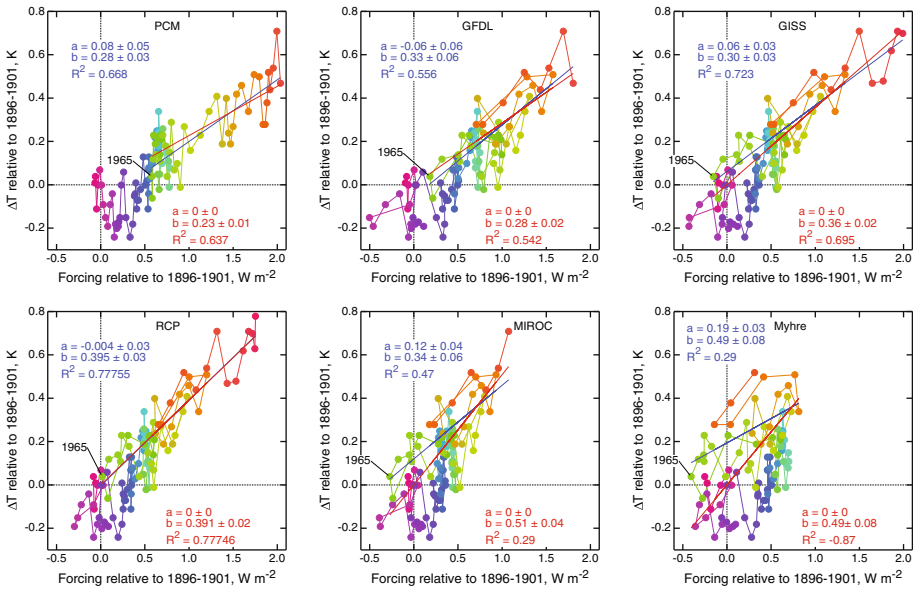


**Fig. 10** Examination of proportionality of surface temperature anomaly and forcing (Eq. 12). Surface temperature anomaly (relative to 1896–1901) is plotted against total forcing from the several forcing data series examined in this study, as convolved with the function  $\exp(-t/3) [1 - \exp(-1/3)]$ . Fits to data in the form  $\Delta T = a + bF$  from 1965 (indicated) to the ends of the several forcing data series are ordinary linear least squares, *blue*, and least squares but with  $a$  held equal to 0, *red*. Also indicated as  $R^2$  is fraction of variance in the original data accounted for by the regression; negative value indicates that variance in the residuals about the regression exceeds that in the temperature data themselves. The *color* coding reflects the date (*violet*, 1896 to *red*, 2009)

forcings adduced by the several modeling groups, differ among the figures. As the hypothesis under examination is that surface temperature has increased in response to the applied forcing, the forcing is taken as the independent (known) variable in computing the regressions. The regressions are restricted to the forcing and temperature data for 1965 and beyond, consistent with the start date of the regression for heating rate, but both the forcing and temperature anomaly data are referenced to the common base period, 1896–1901. However, the entire data sets for forcing and temperature from 1896 to the end of the several forcing data sets are shown, and it would seem from inspection of the graphs that, for most of the forcing data sets, the entire time series is well represented by a linearly proportional relation. In the regressions, a rather robust linear proportionality is exhibited for most of the forcing data sets between surface temperature and forcing, but with different slopes. The fraction of the variance in the temperature data accounted for by the regression forced through the origin is over 50% for four of the six forcing data sets. For most of the data sets, the intercept is near zero; constraining the regression line to pass through the origin results in little decrease in the fraction of the variance in the data accounted for by the regression, denoted  $R^2$  in the figures and in Table 2. (For the 2-parameter fits  $R^2$  is equal to the square of the Pearson product-moment regression coefficient, as usual; for the 1-parameter fits the quantity denoted  $R^2$  is explicitly evaluated from the residuals; the value of  $R^2$  for the 2-parameter fit necessarily exceeds that for the 1-parameter fit.) A high correlation with zero intercept, that is, temperature anomaly proportional to forcing (Eq. 12), is consistent with a planetary heating rate  $N$  that is

**Table 2** Equilibrium climate sensitivity  $S_{eq}$  and transient sensitivity  $S_{tr}$  and other quantities determined for the several forcing data sets examined in this study

Method	Quantity	Unit	Forcing data set						Relative range
			PCM	GFDL	GISS	RCP	MIROC	Myhre	
	$F(1900-1990)$	$W\ m^{-2}$	2.1	1.9	1.6	1.6	1.1	1.0	0.69
$F-N$	$S_{eq}$	$K\ (W\ m^{-2})^{-1}$	0.30	0.39	0.59	0.70	–	–	0.82
	$\sigma(S_{eq})$	$K\ (W\ m^{-2})^{-1}$	0.02	0.03	0.04	0.02	–	–	
	$R^2$		0.52	0.25	0.50	0.58	–0.97	–2.9	
	$\Delta T_{2\times}$	K	1.10	1.45	2.19	2.60	–	–	0.82
	$\sigma(\Delta T_{2\times})$	K	0.07	0.12	0.14	0.15	–	–	
$\kappa$	$S_{tr}$	$K\ (W\ m^{-2})^{-1}$	0.23	0.28	0.36	0.39	0.51	–	0.79
	$\sigma(S_{tr})$	$K\ (W\ m^{-2})^{-1}$	0.01	0.02	0.02	0.02	0.04	–	
	$R^2$		0.64	0.54	0.69	0.78	0.29	–0.87	
	$S_{eq}$	$K\ (W\ m^{-2})^{-1}$	0.31	0.43	0.63	0.74	1.32	–	1.61
	$\sigma(S_{eq})$	$K\ (W\ m^{-2})^{-1}$	0.02	0.04	0.06	0.07	0.31	–	
	$\Delta T_{2\times}$	K	1.16	1.60	2.32	2.75	4.90	–	1.61
	$\sigma(\Delta T_{2\times})$	K	0.09	0.16	0.22	0.25	1.15	–	

$S_{tr}$  was evaluated as coefficient of proportionality between temperature anomaly and forcing.  $S_{eq}$  was determined by two methods: directly as coefficient of proportionality between temperature anomaly and forcing minus planetary heating rate ( $F-N$  method), and via  $S_{tr}$ , accounting for the planetary heating rate, as  $S_{eq} = (S_{tr}^{-1} - \kappa)^{-1}$  (Eq. 10) where  $\kappa$  is the coefficient of proportionality between heating rate and temperature anomaly ( $\kappa$  method).  $R^2$  denotes fraction of variance in temperature anomaly data set accounted for by the linear regression with zero intercept. Uncertainties denote 1-sigma estimates inferred from least-squares fits (neglecting autocorrelation), suitably propagated for derived quantities. Relative range denotes range divided by median

likewise proportional to the temperature increase (Eq. 7). The sole exception among the forcing data sets examined to the linear proportionality between surface temperature and forcing is for the forcing data set of Myhre et al. (2001), which exhibits poor correlation and for which constraining the regression line to pass through the origin results in a variance about the regression line that actually exceeds the variance in the temperature data themselves. Thus, the Myhre forcing data set would seem entirely inconsistent with a linear proportionality between observed temperature change and forcing.

### 3.4 Determination of Equilibrium Climate Sensitivity by the $\kappa$ Method

As described above, if the energy imbalance of the planet (net energy flow into the planet) is linearly proportional to the change in temperature, the transient sensitivity (slope of a graph of temperature change versus forcing, Fig. 10) would be related (Eq. 11) to the geophysical quantities  $\kappa$  and  $\lambda$  as  $S_{tr} \equiv (\kappa + \lambda)^{-1}$ . Thus, within this model, for  $\kappa$  independently determined from observations of the change in GMST and rate of change of global heat content (Fig. 6), it is possible to determine the equilibrium sensitivity as  $S_{eq} = (S_{tr}^{-1} - \kappa)^{-1}$ , Eq. 13. These relations are used to evaluate  $S_{eq}$  from the transient sensitivities determined for the several forcing data sets; the results are given in Table 2 as are the corresponding values of the  $CO_2$  doubling temperature. As is the case with the values of the transient sensitivity, the differences in the values of the equilibrium sensitivity determined for the several forcing data sets are due entirely to differences in the forcing data sets. The relative range of the values of the equilibrium climate sensitivity,

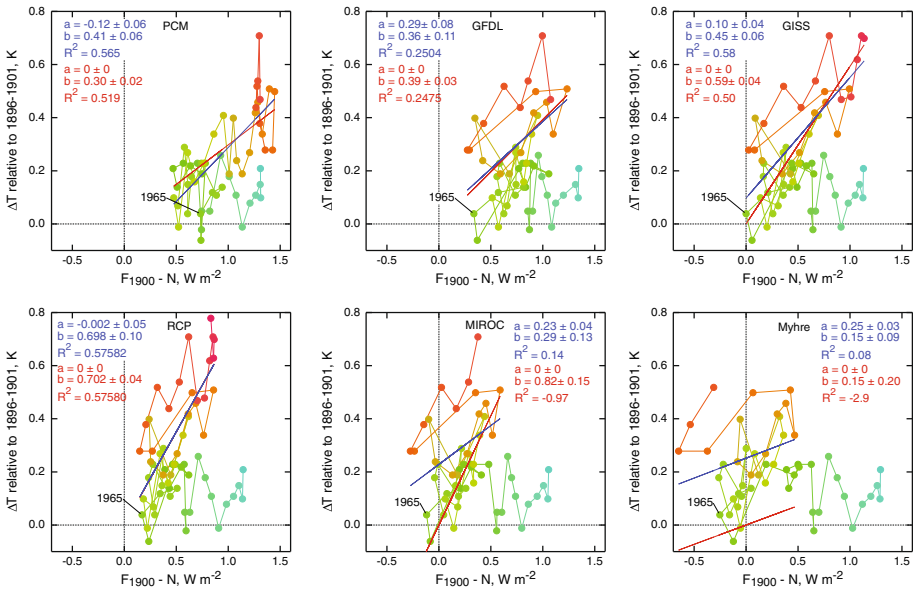


**Fig. 11** Examination of proportionality between temperature anomaly and forcing minus heating rate (Eq. 6). Surface temperature anomaly (relative to 1896–1901) is plotted against  $F-N$ , where  $F$  is total forcing from the several forcing data series examined in this study, as convolved with the function  $\exp(-t/3)$   $[1 - \exp(-1/3)]$ , and  $N$  is planetary heating rate shown in Fig. 4. Data are shown for the entire time period for which ocean heat content data are available, extending to 1949, but regression fits in the form  $\Delta T = a + b(F-N)$  are limited to the time period from 1965 (indicated) to the ends of the individual forcing data series. Fits are ordinary linear least squares, *blue*, and least squares but with the intercept  $a$  held equal to 0 K, *red*. Also indicated as  $R^2$  is fraction of variance in the original data accounted for by the regression; negative value indicates that variance in the residuals about the regression exceeds the variance in the temperature data themselves. The color coding reflecting the date (*light blue*, 1949, to *red*, 2009), is consistent with the color coding of Fig. 9)

123%, is substantially greater than that in the forcings themselves or in the transient sensitivities because of the subtraction involved in the calculation of  $S_{eq}$ .

### 3.5 Determination of Equilibrium Climate Sensitivity from Correlation of Temperature Change with $F-N$

According to Eq. 6, surface temperature anomaly as a function of time would be expected to exhibit a linear proportionality to forcing  $F$  minus planetary heating rate  $N$ , also both functions of time, with slope equal to the equilibrium sensitivity  $S_{eq}$ . This relation was examined by means of graphs of surface temperature anomaly relative to the 1896–1901 base period versus forcing relative to the same period minus heating rate  $N$  for the several forcing data sets, Fig. 11. In these graphs, the time period represented by the data is limited to the period subsequent to 1949, for which heating rate data are available. As the accuracy and representativeness of the ocean heat content data prior to 1965 are questionable, fits to obtain linear regressions were carried out only for the data from 1965 through the ends of the several forcing data sets. Differences in the slopes

among the several graphs are entirely a consequence of the differences in the forcing data sets. As the hypothesis is that surface temperature increases in response to the forcing minus the planetary heating rate, the latter is taken as the independent (known) variable in computing the regressions.

Correlations between  $\Delta T$  and  $F-N$  (see also Table 2) are fairly robust,  $R^2 > 0.5$ , for three (GISS, RCP, and PCM) of the six forcing data sets, with intercepts, corresponding to zero forcing, close to 0 K, and with little decrease in the fraction of the variance accounted for by the regression for the regression line constrained through the origin, indicative of a linearly proportional dependence of  $\Delta T$  on  $F-N$  expected for the energy balance model. In all cases, the  $R^2$  values are less than that exhibited in the regression of heating rate on surface temperature anomaly, 0.68 (Fig. 5), which would seem to indicate that the forcing data introduce additional variance into the relation. For the MIROC and Myhre forcing data sets, only a rather small fraction of the variance is accounted for by the regression, and constraining the regression line to pass through the origin at  $F = 0$  results in the variance about the regression line exceeding the variance characterizing the temperature anomaly data about their mean value; this situation is revealed by a negative value of  $R^2$ , evaluated as the fraction of the variance in the data accounted for by the regression. The departure from linear proportionality should not necessarily be taken as implying that the forcing data do not provide an accurate picture of actual forcing of Earth's radiation balance over this time period, but it would certainly seem that these forcing data, together with the observations of increase in temperature and planetary heating rate, are inconsistent with an energy balance model for which the change in net emitted irradiance at the top of the atmosphere is proportional to the increase in surface temperature.

The values of equilibrium sensitivity determined by the  $F-N$  method would appear to exhibit a much smaller relative range than those determined by the  $\kappa$  method. However, the difference is due entirely to inclusion of the sensitivity determined with the MIROC forcing data in the set of values of  $S_{\text{eq}}$  obtained by the  $\kappa$  method, whereas this data set is excluded from the values of  $S_{\text{eq}}$  obtained by the  $F-N$  method because of failure to exhibit a linear regression. If that value of  $S_{\text{eq}}$  is removed from the set of values obtained by the  $\kappa$  method, the relative range is virtually identical and, indeed, the values of  $S_{\text{eq}}$  by the two methods agree within their one-sigma uncertainties. The identity of the results obtained by the two different methods lends support to the two methods and values obtained.

### 3.6 Estimates of Upper- and Lower-Compartment Time Constants

As the expressions for the time constants of the upper and lower compartments (Eq. 8) involve quantities that are not determined directly in this analysis, it is not possible to explicitly determine values for these time constants. However, algebraic manipulation of the expression for the time constant of the upper compartment yields an expression for  $\tau_s$  as the product of scoping value,  $\tau'_s$ , times two correction factors both of which are near unity, and of opposite sense,

$$\tau_s = \frac{C_U}{\beta + \lambda} = \tau'_s \cdot \frac{C_U}{C_{\text{eff}}} \cdot \frac{\lambda + \kappa}{\lambda + \beta}; \quad \tau'_s = C_{\text{eff}} S_{\text{tr}}.$$

Values of  $\tau'_s$  for the several forcing data sets range from 4 to 9 years, from which it may be concluded that  $\tau_s$  is comparable. By a similar argument,

$$\tau_1 = C_L \left( \frac{1}{\lambda} + \frac{1}{\beta} \right) = \tau'_1 \cdot \left( \frac{\lambda}{\kappa + \lambda} \right) \cdot \left( \frac{\kappa}{\lambda} + \frac{\kappa}{\beta} \right); \tau'_1 = \frac{C_L}{(\kappa - S_{tr} \kappa^2)}.$$

Values of  $\tau'$  for the several data sets range from 400 to 580 years, establishing the long time constant of the lower compartment. These estimates are consistent with the assumed large separation of time constants for the two compartments that is a premise of the model.

## 4 Discussion

### 4.1 Effective Heat Capacity of the Climate System

The graph of ocean heat content anomaly versus temperature anomaly (Fig. 4) gives rise, as a slope, to the effective heat capacity of the ocean that is coupled to the climate system, from which the total effective heat capacity of the climate system was obtained by taking into account other sinks of heat in the climate system. The resulting effective heat capacity  $21.8 \pm 2.1 \text{ W year m}^{-2} \text{ K}^{-1}$  is somewhat greater, and is determined with considerably less uncertainty, than the value given by a similar approach by Schwartz (2007),  $14 \pm 6 \text{ W year m}^{-2} \text{ K}^{-1}$ , a consequence mainly of improved estimates of ocean heat content anomaly subsequent to the study of Levitus et al. (2005) on which the earlier determination was based. However, this uncertainty reflects only scatter about the regression line and does not encompass systematic uncertainty that would result from inadequate sampling and methodological artifacts in the heat content measurements. As determination of this effective heat capacity does not rely on modeled forcings, it is not subject to uncertainties in the forcings and therefore is entirely observationally determined. In an analysis of ocean uptake in climate model runs with the Hadley Centre coupled atmosphere–ocean general circulation model (AOGCM) in which the  $\text{CO}_2$  mixing ratio was increased by  $1\% \text{ year}^{-1}$ , compounded, Gregory (2000) found an increase in ocean heat content of  $7.5 \times 10^{23} \text{ J}$  for a temperature increase of 1.8 K, from which a heat capacity of  $25.9 \text{ W year m}^{-2} \text{ K}^{-1}$  may be inferred. Based on climate model studies in which model parameters were allowed to vary, Frame et al. (2005) presented values (0.1–2.05)  $\text{GJ m}^{-2} \text{ K}^{-1}$  (5–95% confidence), equivalent to (3.2–65)  $\text{W year m}^{-2} \text{ K}^{-1}$ , a range that encompasses the value obtained here but provides little constraint or insight. Andrews and Allen (2008) present an analysis of this quantity as inferred from studies with coupled AOGCMs yielding a probability distribution function (PDF) for this quantity that peaks at about  $0.7 \text{ GJ m}^{-2} \text{ K}^{-1}$  (principal contribution to the PDF between 0.4 and  $1.4 \text{ GJ m}^{-2} \text{ K}^{-1}$ ; equivalently,  $22 \text{ W year m}^{-2} \text{ K}^{-1}$ ; range 13–44  $\text{W year m}^{-2} \text{ K}^{-1}$ ), broadly consistent with the observationally determined heat capacity found here.

Although the analysis of the ocean heat content observations presented here provides a fairly tight constraint on the effective heat capacity, interpretation of the physical meaning of this quantity remains problematic. As the determination is based on the increase in heat content of the entire ocean (and other tightly coupled components of the climate system), the resulting heat capacity is not the heat capacity just of the upper compartment of the climate system but accounts for the increase in heat content in the deeper compartment as well; the penetration of heat into the deep ocean occurs in conjunction with downwelling ocean circulations (Levitus et al. 2005). Still, this effective heat capacity is certainly well less than the heat capacity of the deep ocean, which is an order of magnitude greater. Insight into the multiple response times of the climate system from a two-compartment model is provided by Held et al. (2010), and a more thorough interpretation through an

upwelling diffusion model is provided by Hoffert et al. (1980). An approach to separating the shallow ocean compartment from the deep ocean compartment was advanced by Gregory (2000), who examined temporal autocorrelation of temperature as a function of depth with that in the top ocean layer in output of the Hadley Centre AOGCM, finding a sharp break at about 100 m, for which the heat capacity, expressed per area of planet would be  $0.28 \text{ GJ m}^{-2} \text{ K}^{-1}$  ( $9.0 \text{ W year m}^{-2} \text{ K}^{-1}$ ). It would seem that a similar, observationally based approach might usefully distinguish the upper and lower oceanic compartments of the actual climate system. In this respect, attention is called to a time series of measurements of ocean temperature as a function of depth (surface to 800 m) over a 15-year period (Sutton and Roemmich 2001) that shows the damping of the amplitude of the seasonal cycle of temperature with depth from about 6 K peak-to-peak at the surface to about 1 K at 150 m, suggesting an observational approach to determining the time-dependent penetration of heat due to a secular change in surface temperature induced by changing atmospheric composition.

#### 4.2 Heat Uptake Coefficient

The heat uptake coefficient  $\kappa$ , the rate of heat uptake by the planet normalized to the global temperature anomaly was determined as the slope of the linear proportionality between the rate of increase of ocean heat content, evaluated as the time derivative of the ocean heat content, augmented to include estimates of additional heat sinks, and the surface temperature anomaly. This heat uptake coefficient is  $1.05 \pm 0.06 \text{ W m}^{-2} \text{ K}^{-1}$ , where again the uncertainty characterizes the regression but not systematic errors in the heat content data. For the observed increase in global temperature relative to 1900  $\Delta T_{\text{obs}} = 0.78 \text{ K}$  in 2010 (Hansen et al. 2010, as extended at <http://data.giss.nasa.gov/gistemp/>), this value of  $\kappa$  would indicate a heat flux into the climate system, which is equal to the energy imbalance of the climate system, of  $0.82 \text{ W m}^{-2}$ . Such an energy imbalance is consistent with the present heating rate shown in Fig. 5 (from which it is derived) and with other current observationally based estimates of this quantity (Palmer et al. 2010; Lyman 2011).

As with the effective heat capacity, the heat uptake coefficient is wholly observationally determined. Further, it would seem that this heat uptake coefficient is an intrinsic property of Earth's climate system, rather than a property that is dependent on the nature and/or magnitude of recent forcings. Certainly, a proportionality between the rate of heat input into the climate system and the increase in global temperature following imposition of a radiative forcing would not be maintained indefinitely, as the system approaches its ultimate new steady state. Nonetheless at least in the early years following the onset of forcing, and even more, in situations of continuously increasing forcing, the linear proportionality between the rate of increase of heat content and the temperature anomaly would seem to be a useful means of quantifying the heat input into the climate system and the consequences of the departure from steady state following imposition of the forcing.

Despite considerable interest in the heat uptake coefficient in interpreting climate model calculations (Gregory and Forster 2008; Dufresne and Bony 2008), there does not seem to be prior observationally based determination of this quantity. Gregory and Forster determined  $\kappa$  as the slope of a regression of net heat flux into the planet, relative to control runs, against GMST anomaly in the output of 16 AOGCMs that participated in the intercomparison of models over the twentieth century carried out by the IPCC (2007) Fourth Assessment, the same approach as employed here with observation-derived data. For the 16 models examined, the mean value of  $\kappa$  was  $0.62 \pm 0.13$  (1 sigma); maximum 0.83; minimum 0.41. It would thus seem that the heat uptake coefficient may be somewhat

underestimated in current climate models. For a given equilibrium sensitivity, an underestimate would result in the rate of increase in GMST being overestimated in climate model calculations. As the net heat flux is subtractive from the forcing in determining the rate of temperature increase, the magnitude of the overestimate would depend on the forcing. Alternatively, knowledge of the heat transfer coefficient might be used to infer the equilibrium sensitivity of a climate model from  $S_{tr}$  obtained from the dependence of modeled temperature anomaly on forcing ( $\kappa$  method, Eq. 11); as  $\kappa$  is subtractive from  $S_{tr}^{-1}$ , an erroneously low value of  $\kappa$  would result in an overestimate of  $S_{eq}$ , the magnitude of which would depend on the value of  $S_{tr}^{-1}$ .

As with the effective heat capacity, it would seem that questions remain regarding the interpretation of this heat flux. Both observationally and from the climate model output, the quantity that is determined is the total net heat flux into the planet, normalized to the global temperature anomaly, whereas the heat flux that is calculated in two-compartment models is the heat flux from the upper, short-time-constant compartment to the lower, long-time-constant compartment. As the upper compartment undoubtedly comprises a substantial fraction of the effective heat capacity of the system, it would seem fruitful to more explicitly distinguish between the two compartments in refining these concepts in future work. Nonetheless, it is clear that the net heat flux into the climate system that is subtractive from the applied forcing to yield the equilibrium sensitivity of the climate system, Eq. 6, is the heat flux into the entire climate system. The observationally based finding of a linear proportionality between heat flux and temperature anomaly supports the relation between transient and equilibrium sensitivities, Eq. 13 that can be used to infer the equilibrium sensitivity from the transient sensitivity based on observations (and assumed forcings) or to infer the transient sensitivity from climate model runs that yield the equilibrium sensitivity with slab-ocean models.

#### 4.3 Transient and Equilibrium Climate Sensitivities

This study has examined the relation between observed increase in GMST and forcing, as calculated by several groups, in terms of a two-compartment energy balance model. According to this model, a linear proportionality would be expected between the two quantities, the slope of which would be interpreted as a transient climate sensitivity  $S_{tr}$ . This expectation is borne out for five of the six forcing data sets examined, for forcing and temperature anomaly over the twentieth century. However, the regression slopes (limited to measurements subsequent to 1965) differ for the several forcing data sets by amounts that substantially exceed the uncertainties in the regression slopes (Table 2) and by amounts that are significant in the context of interpretation of climate change over the twentieth century. Recognition that the planetary heating rate  $N$  is subtractive from the forcing  $F$  to yield the equilibrium sensitivity  $S_{eq}$  suggests a further linear proportionality between GMST anomaly and  $F-N$ , the proportionality constant being  $S_{eq}$ , leading to determination of  $S_{eq}$  as this slope, the  $F-N$  method. A linear proportionality was found for four of the six data sets examined; again the sensitivities so determined differ by amounts that substantially exceed the uncertainties in the regressions and that are important in the context of understanding climate change. The finding of a linear proportionality between the heating rate and GMST anomaly yielding the heat uptake coefficient  $\kappa$  permits determination of  $S_{eq}$  from  $S_{tr}$ , the  $\kappa$  method. This method yielded values of  $S_{eq}$  for the five forcing data sets for which it was possible to determine  $S_{tr}$ . The values of  $S_{eq}$  so determined agreed closely with the values of  $S_{eq}$  determined by the  $F-N$  method. Here, it should be



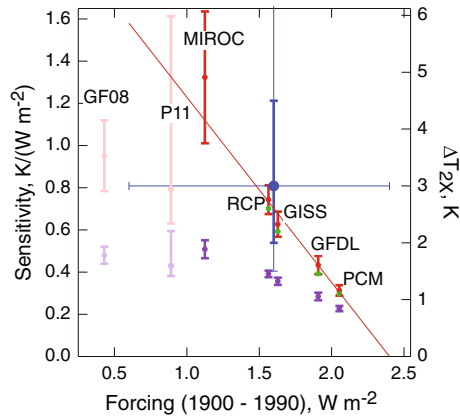


**Fig. 12** Dependence of transient climate sensitivity  $S_{tr}$ , Eq. 10, (purple) and equilibrium climate sensitivity  $S_{eq}$  inferred by the  $F-N$  method, Eq. 6, (green) and by the  $\kappa$  method, Eq. 11, (red) on forcing between 1900 and 1990. Uncertainties in equilibrium sensitivity (shown for the  $\kappa$  method) represent one sigma, estimated by error propagation from the uncertainties in  $S_{tr}$  (also shown, one sigma) and  $\kappa$ . Right axis gives equivalent  $\text{CO}_2$  doubling temperature evaluated from  $S_{tr}$ , or  $S_{eq}$ . Also shown are  $S_{tr}$ , determined by Gregory and Forster (2008) and Padilla et al. (2011) and  $S_{eq}$  evaluated from those values of  $S_{tr}$  using the value of  $\kappa$  determined here, with associated one-sigma uncertainties. Shown in blue are best estimates of equilibrium climate sensitivity and anthropogenic forcing (relative to preindustrial) and associated uncertainties as given by the IPCC Fourth Assessment Report (2007); thick uncertainty lines correspond to central 66% of the likelihood function (roughly equivalent to one sigma); thin uncertainty lines denote “very likely” range corresponding to the central 90% of the likelihood function. Red line denotes extrapolation of equilibrium sensitivities to the full “very likely” range of forcing given by the 2007 IPCC assessment

emphasized that the absence of linear proportionality between GMST anomaly and forcing for a single forcing data set of the six examined (that of Myhre et al. 2001) does not demonstrate those forcing data are an inaccurate representation of forcing over the latter part of the twentieth century but only that these forcing data are inconsistent with the energy balance model considered. This inconsistency in a single forcing data set, and more broadly the differences in the sensitivities determined from the several forcing data sets examined, underscore the importance of accurate determination of climate forcing over the twentieth century, especially the latter part of the twentieth century for which ocean heat content data are available, to observational determination of Earth’s climate sensitivities.

Values of the equilibrium sensitivities were determined for five of the six forcing data sets examined, all of which are within the “very likely” range<sup>2</sup> given for this forcing by the IPCC (2007) Assessment. These sensitivities range from  $0.31\text{--}1.32\text{ K (W m}^{-2}\text{)}^{-1}$ , corresponding to  $\Delta T_{2\times}$   $1.2\text{--}4.9\text{ K}$ , and, with the exception of the MIROC forcing data set, are less than the best estimate,  $3\text{ K}$  given for this quantity by the 2007 IPCC Assessment, Fig. 12. Two of the five forcing data sets yield sensitivities within the IPCC “likely” range (see Footnote 2),  $2\text{--}4.5\text{ K}$ , with two below and one (MIROC) above this range, although the large uncertainty attached to the latter extends well into this range. For the PCM and GFDL forcing data sets, the equilibrium sensitivities are below the lower bound of the “likely” range for this quantity, and indeed are nearly at, or below, the limit of the “very likely” range for this quantity,  $\Delta T_{2\times} = 1.5\text{ K}$ .

<sup>2</sup> Here the term “very likely” is used in the sense of the 2007 IPCC Assessment Report; that is, corresponding to the estimate of the central 90% of the PDF for the quantity. Likewise the term “likely” is used to denote the estimate of the central 66% of the PDF.

Examination of the relation between the values of  $S_{\text{ir}}$  and  $S_{\text{eq}}$  determined by this analysis and the twentieth century climate forcing used to infer the sensitivity from the observed increase in GMST (Fig. 12) shows distinct anticorrelation, that is, a low forcing yields a high sensitivity, and vice versa. An anticorrelation between forcing and sensitivity, which would be expected for a given increase in GMST has been noted previously in both empirical inference (Gregory et al. 2002; Schwartz 2004) and in analysis of the equilibrium sensitivity of climate models (Kiehl 2007; Knutti 2008). Of course the equilibrium climate sensitivity, which is a property of Earth's climate system, cannot depend on the forcing. Rather it is the equilibrium climate sensitivities that are inferred from estimates of the forcing that exhibit such dependence. The anticorrelation between inferred equilibrium sensitivity and forcing found here indicates that the only way that Earth's equilibrium climate sensitivity could be as great as the central value of the IPCC estimate,  $\Delta T_{2\times} = 3$  K, would be for the total forcing (recall that the forcing corresponds to the period 1900–1990) to be about  $0.8 \text{ W m}^{-2}$ . Such a low forcing, which is at the low end of the IPCC “very likely” range, would require a rather large negative aerosol forcing to offset the forcing, by the well mixed greenhouse gases, about  $2.3 \text{ W m}^{-2}$  in 1990; here, it must be emphasized that this is not an “inverse” calculation of aerosol forcing, as would be obtained by using a modeled sensitivity, but rather an observational constraint on this forcing together with the best estimate of the equilibrium climate sensitivity given by the IPCC assessment. Extrapolation of the anticorrelation between equilibrium sensitivity and forcing to the entire span of the “very likely” range for the total forcing given by the IPCC 2007 assessment ( $0.6\text{--}2.4 \text{ W m}^{-2}$ ) yields a range in equilibrium sensitivity from near zero to  $1.6 \text{ K (W m}^{-2}\text{)}^{-1}$  ( $\Delta T_{2\times} = 6$  K). This wide range of equilibrium climate sensitivity underscores the importance of constraining the forcing if the climate sensitivity is to be determined with accuracy, either observationally or in climate model studies.

Relevant prior studies examining the relation of observed temperature change to forcing are of Gregory and Forster (2008) and Padilla et al. (2011). Gregory and Forster presented, for forcing determined by the Hadley Centre climate model, graphs of observed temperature change versus anthropogenic forcing or versus total forcing; years strongly influenced by volcanic emissions were excluded from determination of the regression slope. The transient sensitivity found in that study as the slope of a regression of  $\Delta T$  observed over the years 1970–2006 against “median” estimates of total forcing by anthropogenic greenhouse gases and aerosols (years strongly affected by volcanic aerosols excluded) was  $0.48 \pm 0.04 \text{ K (W m}^{-2}\text{)}^{-1}$ ; the corresponding value of equilibrium sensitivity, evaluated with the value of  $\kappa$  determined here is  $0.95 \pm 0.18 \text{ K (W m}^{-2}\text{)}^{-1}$  ( $\Delta T_{2\times} = 3.5$  K). Padilla et al. used a statistical approach to infer the quantity denoted here as  $\kappa + \lambda$  from the observed temperature record together with an composite forcing based on the forcings from the GISS, GFDL, and Gregory-Forster forcing data sets. The resulting transient sensitivity was  $0.43 (+0.16; -0.05) \text{ K (W m}^{-2}\text{)}^{-1}$ . For the value of  $\kappa$  determined in this study, the corresponding equilibrium sensitivity is  $0.79 (+0.82; -0.16) \text{ K (W m}^{-2}\text{)}^{-1}$ . The sensitivities determined in those studies are somewhat to substantially greater than the values determined for the forcing data sets examined here, Fig. 12. Correspondingly, the total forcings over the twentieth century employed in these analyses were lower to considerably lower,  $0.89$  and  $0.43 \text{ W m}^{-2}$ , than those obtained with the forcings from the studies examined here; the forcing data set employed by Gregory and Forster is less even than the lower bound of the “very likely” range for forcing up to 2005 as given by the IPCC, although that gap is closed by the incremental forcing between 1990 and 2005. As also found here, the Padilla et al. analysis indicates that the transient sensitivity differed for the several forcings; however, for the three forcings examined by Padilla et al., the range of

the central values of the transient sensitivities,  $0.43\text{--}0.53 \text{ K (W m}^{-2}\text{)}^{-1}$ , was considerably narrower than found in the present study and not monotonic with the forcings.

#### 4.4 Climate System Time Constants

Although the estimates of time constants for relaxation of perturbations in heat content of the two compartments of the climate system determined by this analysis depend on the magnitudes of the forcings of the several data sets examined, for each of the forcing data sets, the values associated with the two compartments are clearly separated into a short time constant (median 6.3 year, range 4.1–9.2 years) and a long time constant (median 470 year, range 400–580 year). A rapid initial response to a step-function forcing that exhibits most of the climate system response followed by a further response of lower magnitude and long duration is widely exhibited in coupled climate model runs (Brasseur and Roeckner 2005; Matthews and Caldeira 2007; Knutti et al. 2008; Held et al. 2010; Hansen et al. 2011; Knutti and Plattner 2012). Examining a two-compartment model having parameters chosen to match experiments with the Hadley Centre climate model, Gregory (2000) found that the response could be characterized by a short time constant of about 12 year and as second time constant at least an order of magnitude greater. Boucher and Reddy (2008) found that the response of GMST in the HadCM3 climate model to a forcing that was rapidly ramped up and then held constant was accurately approximated by a two-exponential function with time constants 8.4 and 410 years. A large gap in time constants was noted also by Held et al. (2010), in an analysis of the response of the GFDL climate model to step-function changes in forcings, with a short time constant characterizing the transient response of the climate system to an applied forcing and a much longer response time, which they characterize as “centuries or longer” associated with the second, large-heat-capacity compartment of the climate system. Based on an analysis of model runs of two AOGCMs and a model of intermediate complexity run out to equilibrium Jarvis and Li (2011) likewise find two discrete time scales, one of about 20 years and a second of about 700 years. Based on an examination of transient runs across the climate models that participated in the intercomparison reported in the 2007 IPCC Assessment, Lucarini and Ragone (2011) characterized the longer relaxation time as of order 500–700 years.

A response of Earth’s climate system to perturbations that is characterized by two such widely separated time constants would have important implications for the interpretation of climate change over the past half century during which forcing has likely been systematically increasing. Specifically, for such a situation, the response of GMST to the forcing would be in rather close steady state to the forcing, lagging the response given by the transient sensitivity by about one time constant, that is, just a few years. Thus, Held et al. (2010) found that the response of the GFDL model to twentieth century forcing is accurately matched by a single-box model with a time constant of 4 year and a transient sensitivity of  $0.43 \text{ K (W m}^{-2}\text{)}^{-1}$ . Ultimately, Held et al. found that the heat input into what they term the “recalcitrant” compartment of the climate system becomes appreciable, but under a situation of continuously increasing forcing, the increase in temperature of this compartment remains a small fraction of that of the short-time-constant compartment. On the time scale certainly of several decades, it would seem that the increase in temperature of the deep ocean is insufficient to appreciably diminish the proportionality between temperature anomaly and heat flux. In other words, the response of the climate system to forcing would continue to be given by the transient sensitivity, not the equilibrium sensitivity. This situation would likely continue to hold as temperature anomaly continues to increase. A departure from proportionality between temperature anomaly and heat flux to

the long-time-constant compartment might be expected only after some decades of constant forcing, at which point the back flux of heat from the deep ocean compartment to the shallow ocean compartment would begin to become appreciable. Based on these considerations it would seem that the most relevant measure of climate sensitivity for policy purposes is the transient sensitivity, as it is this sensitivity that will govern climate system response to changes in forcing, given that the time constant for the deep ocean compartment to respond to forcings is several centuries.

#### 4.5 Concerns with this Analysis

This analysis consists of three distinguishable components, listed here in order of increasing dependence on assumptions:

1. Determination of  $C_{\text{eff}}$  and  $\kappa$ . Determination of these quantities rests entirely on measurements (temperature, ocean heat content) and is independent of details of the two-compartment model or of assumptions about the forcings over the twentieth century.
2. Determination of  $S_{\text{tr}}$  and  $S_{\text{eq}}$ . Determination of these quantities rests on the assumed first-order response of GMST to forcing, or equivalently, on a linear response of net irradiance at the TOA to change in GMST. The existence of two distinguishable sensitivities rests on the climate system being characterized by two (or more) distinguishable compartments with widely separated response times, but is independent of the details of the two-compartment model. Determination of both sensitivities depends also on choice of the forcing data set.
3. Estimation of  $\tau_s$ ,  $\tau_l$ . In addition to dependence on the above assumptions and input data, determination of these quantities depends explicitly also on the climate system being represented by a two-compartment model.

A source of possible error, affecting determination of  $C_{\text{eff}}$  and  $\kappa$ , and hence of all the quantities determined here, is error in the increase in planetary heat content inferred here from the increase of heat content of the world ocean, and in turn in the planetary energy imbalance, the time derivative of the heat content. Ocean heat content is subject to uncertainty in the measurements, arising from changes in methods and limited and nonuniform sampling (geographically and as a function of depth) over the period of record, as discussed by Lyman (2011). A greater rate of heat uptake would result in a greater inferred equilibrium climate sensitivity than that determined here, and conversely a smaller rate of heat uptake would result in an even lower equilibrium sensitivity, demonstrating the importance of this quantity also in determining equilibrium climate sensitivity. An inherent limitation to this approach is that it requires determining the rate of heat uptake as a time derivative of the ocean heat content with the attendant requirements on precision and the associated requirement of measurements over an extended time period before the derivative can be inferred with confidence. An alternative approach to determining heat imbalance is through satellite measurements of the net flux at the top of the atmosphere. As discussed by Stevens and Schwartz (2012) an improvement in measurement accuracy of more than an order of magnitude is required to yield an accuracy that is comparable to that of the heat content measurements.

Determination of Earth's climate sensitivities and compartment time constants is a hybrid based on largely modeled forcings in addition to observations. Determination of the transient sensitivity depends on GMST anomaly, which is known with considerable confidence from multiple independent determinations (NASA GISS, Hansen et al. 2010; NOAA, Smith et al. 2008; Climatic Research Unit, UK, Brohan et al. 2006). The

equilibrium sensitivity depends also on  $\kappa$ , as discussed above. Forcings are obtained by model-based calculations of the radiative influence of measured or modeled perturbations of atmospheric composition (gases and aerosols). The dependence on choice of forcing data set is explicitly examined. Clearly, the several forcings employed in this analysis, which are characteristic of present understanding and uncertainty, cannot all be correct, and the strong dependence of the inferred climate sensitivity to the forcing employed in the analysis underscores the importance of determining forcing with greater accuracy if climate sensitivity is to be determined with confidence (Schwartz 2004; Schwartz et al. 2010).

As the analysis presented here rests entirely on the assumed independence of normalized climate system response, as manifested in change in net TOA irradiance per forcing, to the nature and geographical distribution of the forcing and to the constancy of this response at least over the time period for which the data are available. Clearly, such constancy of climate system response to forcing must at best be an approximation to the actual climate system response; any departure from this assumption would weaken the conclusions drawn here. Support for this approach comes from linear dependence of change in GMST on forcing, with sensitivity independent of the nature of the forcing, which has been found in numerous model studies, with efficiencies (response per forcing, relative, for example to response to CO<sub>2</sub> forcing) typically within 20% (e.g. Hansen et al. 1997; Joshi et al. 2003; Kloster et al. 2010).

A potential basis for non-constancy of climate sensitivity in a given model (or in the real world) would be a dependence of feedback processes on locus of temperature change, under the expectation that certain geographical regions would exhibit greater or lesser feedbacks than others. Ultimately, such a model fails if, for example, there are local feedbacks such as melting of surface ice that amplify the effects of forcings in one location relative to another. This hypothesis was examined in a coupled climate model study by Boer and Yu (2002), who found that the spatial distribution of temperature response generally exhibited what the investigators denoted a “generic” pattern independent of spatial distribution of the forcing rather than being characteristic of the forcing patterns themselves and leading therefore to only weak dependence of the forcing on the nature or spatial distribution of the forcing. That study noted as well that the patterns of temperature change exhibited “a remarkable linearity or additivity” whereby the sum of response patterns for different forcings was very similar to that for the sum of the forcings. In contrast, also in calculations with coupled models, Watterson and Dix (2005) found that the equilibrium sensitivity, evaluated by the equivalent of the present Eq. 6, varied by as much as  $-20$  to  $+70\%$  compared with a standard doubled CO<sub>2</sub> case, depending on whether forcing was confined to either low- or high-latitude regions, raising caution over the assumption inherent in the sensitivity concept that an increase in GMST depends only on global mean forcing independent of geographical distribution.

Finally, although it might be granted that the analysis such as the present one that is based on measurements of the transient response of the climate system to imposed forcing is capable of yielding information about the transient sensitivity of Earth’s climate system, the question might nonetheless be raised whether such an analysis is capable of yielding information pertinent to the equilibrium sensitivity, which would be approached only after 1,000 years or more. Here, it should be recalled that the equilibrium sensitivity is as defined here, and generally, is a property of Earth’s present climate system in the sense that a derivative of a mathematical function is a temporally local property of that function. This temporally local approach to the determination of the equilibrium sensitivity is rooted in Eq. 6 which displays the relation of equilibrium sensitivity to values of forcing, net energy imbalance, and temperature change at any given time.

## 5 Summary and Conclusions

The present analysis has examined several relations among global mean quantities pertinent to climate change: ocean heat content with temperature anomaly (slope, effective heat capacity of the climate system); global heating rate with surface temperature anomaly (slope, heat uptake coefficient); surface temperature anomaly with forcing over the twentieth century (slope, transient climate sensitivity); and surface temperature anomaly with forcing minus heating rate (slope, equilibrium climate sensitivity). Six published estimates of forcing over the twentieth century were examined. The first two relations, yielding effective heat capacity and heat uptake coefficient, are independent of the forcings and thus do not encompass any model-based uncertainty associated with the forcings, allowing determination of the effective planetary heat capacity and the heat uptake coefficient from measurements of global mean surface temperature anomaly and ocean heat content anomaly over the second half of the twentieth century. All of these relations, and for the relations involving forcings, for most of the forcings examined, exhibited robust linear proportionality (i.e., zero intercept in linear regression; in the case of heat capacity, linear relation), consistent with expectation based on an energy balance model of the climate system. Additionally, a second method was applied for evaluating equilibrium climate sensitivity using the heat uptake coefficient that yielded values essentially identical to those of the direct regression.

The results of these correlations are interpreted in terms of a two-compartment energy balance model of Earth's climate system that is characterized by an upper, small-heat-capacity, short-time-constant compartment that corresponds to the atmosphere and upper ocean and a lower, large-heat-capacity, long-time-constant compartment that corresponds to the deep ocean, which is only weakly coupled to the upper compartment. This model leads to a distinction between a transient climate sensitivity, which pertains to the upper compartment, and an equilibrium climate sensitivity, which pertains to the entire climate system including the deep ocean. The analysis leads to estimates of the time constants of the two compartments, which are dependent on the forcing data sets employed, but which are quite separated from one another, about 5 years for the upper compartment, and about 500 years for the lower compartment. In this situation, the response of the climate system to forcings over the twentieth century is governed by the short time constant of the upper compartment, which is the time constant that governs the relation between forcing and surface temperature anomaly. The proportionality between forcing and temperature anomaly exhibited for all but one of the forcing data sets examined, together with the large separation in time constants, supports the transient climate sensitivity, evaluated as the proportionality coefficient of these two quantities, as the measure of Earth's climate sensitivity pertinent to interpreting climate change over the twentieth century and to informing policy decisions about future emissions.

The analysis presented here, although focusing on observational data, nonetheless rests heavily on the forcings over the twentieth century as calculated by several modeling groups based, ultimately, on measured or modeled changes in atmospheric composition. Of these, the forcing due to anthropogenic aerosols is the source of the greatest uncertainty, and it is this uncertainty that is mainly responsible for the differences in forcings over the twentieth century. Confident determination of Earth's climate sensitivities thus remains hostage to accurate determination of these forcings.

**Acknowledgments** I thank the several modeling groups for providing the forcing data sets employed in this analysis. An earlier version of this paper was presented at the Workshop on Observing and Modelling

Earth's Energy Flows organized and sponsored by the International Space Science Institute in Bern Switzerland, January, 10–14, 2011, and I thank Lennart Bengtsson for his encouragement of this study. This study benefited from comments by Bjorn Stevens and a second, anonymous reviewer. This work was supported by the U.S. Department of Energy's Atmospheric System Research Program (Office of Science, OBER) under Contract No. DE-AC02-98CH10886.

## References

- Allen MR, Frame DJ (2007) Call off the quest. *Science* 318:582–583. doi:[10.1126/science.1149988](https://doi.org/10.1126/science.1149988)
- Andrews DG, Allen MR (2008) Diagnosis of climate models in terms of transient climate response and feedback response time. *Atmos Sci Lett* 9:7–12. doi:[10.1002/asl.163](https://doi.org/10.1002/asl.163)
- Andrews T, Forster PM, Gregory JM (2009) A surface energy perspective on climate change. *J Clim* 22(10):2557–2570. doi:[10.1175/2008JCLI2759.1](https://doi.org/10.1175/2008JCLI2759.1)
- Baker MB, Roe GH (2009) The shape of things to come: why is climate change so predictable? *J Clim* 22:4574–4589. doi:[10.1175/2009JCLI2647.1](https://doi.org/10.1175/2009JCLI2647.1)
- Boer GJ, Yu B (2002) Climate sensitivity and climate state. *Clim Dyn* 21:167–176. doi:[10.1007/s00382-003-0323-7](https://doi.org/10.1007/s00382-003-0323-7)
- Boer GJ, Stowasser M, Hamilton K (2007) Inferring climate sensitivity from volcanic events. *Clim Dyn* 28:481–502. doi:[10.1007/s00382-006-0193-x](https://doi.org/10.1007/s00382-006-0193-x)
- Boucher O, Reddy MS (2008) Climate trade-off between black carbon and carbon dioxide emissions. *Energy Policy* 36:193–200. doi:[10.1016/j.enpol.2007.08.039](https://doi.org/10.1016/j.enpol.2007.08.039)
- Brasseur GP, Roeckner E (2005) Impact of improved air quality on the future evolution of climate. *Geophys Res Lett* 32:L23704. doi:[10.1029/2005GL023902](https://doi.org/10.1029/2005GL023902)
- Brohan P, Kennedy JJ, Harris I, Tett SFB, Jones PD (2006) Uncertainty estimates in regional and global observed temperature changes: a new dataset from 1850. *J Geophys Res* 111:D12106. doi:[10.1029/2005JD006548](https://doi.org/10.1029/2005JD006548)
- Cleveland WS, Devlin SJ (1988) Locally-weighted regression: an approach to regression analysis by local fitting. *J Am Stat Assoc* 83(403):596–610. doi:[10.2307/2289282](https://doi.org/10.2307/2289282)
- Collins WD, Ramaswamy V, Schwarzkopf MD, Sun Y, Portmann RW, Fu Q, Casanova SEB, Defresne J-L, Fillmore DW, Forster PMD, Galin VY, Gohar LK, Ingram WJ, Kratz DP, Lefebvre M-P, Li J, Marquet P, Oinas V, Tsushima T, Uchiyama T, Zhong WY (2006) Radiative forcing by well-mixed greenhouse gases: estimates from climate models in the IPCC AR4. *J Geophys Res* 111:D14317. doi:[10.1029/2005JD006713](https://doi.org/10.1029/2005JD006713)
- Domingues CM, Church JA, White NJ, Gleckler PJ, Wijffels SE, Barker PM, Dunn JR (2008) Improved estimates of upper-ocean warming and multi-decadal sea-level rise. *Nature* 453:1090–1093. doi:[10.1038/nature07080](https://doi.org/10.1038/nature07080)
- Duffresne J-L, Bony S (2008) An assessment of the primary sources of spread of global warming estimates from coupled atmosphere-ocean models. *J Clim* 21:5135–5144. doi:[10.1175/2008JCLI2239.1](https://doi.org/10.1175/2008JCLI2239.1)
- Forster PMF, Gregory JM (2006) The climate sensitivity and its components diagnosed from earth radiation budget data. *J Clim* 19:39–52. doi:[10.1175/JCLI3611.1](https://doi.org/10.1175/JCLI3611.1)
- Forster PMD, Taylor KE (2006) Climate forcings and climate sensitivities diagnosed from coupled climate model integrations. *J Clim* 19:6181–6194. doi:[10.1175/JCLI3974.1](https://doi.org/10.1175/JCLI3974.1)
- Frame DJ, Booth BBB, Kettleborough JA, Stainforth DA, Gregory JM, Collins M, Allen MR (2005) Constraining climate forecasts: the role of prior assumptions. *Geophys Res Lett* 32:L09702. doi:[10.1029/2004GL022241](https://doi.org/10.1029/2004GL022241)
- Gouretski V, Reseghetti F (2010) On depth and temperature biases in bathythermograph data: development of a new correction scheme based on the analysis of global ocean data. *Deep-Sea Res* 57:812–833. doi:[10.1016/j.dsr.2010.03.011](https://doi.org/10.1016/j.dsr.2010.03.011)
- Gregory JM (2000) Vertical heat transports in the ocean and their effect on time-dependent climate change. *Clim Dyn* 16:501–515. doi:[10.1007/s003820000059](https://doi.org/10.1007/s003820000059)
- Gregory JM, Forster PM (2008) Transient climate response estimated from radiative forcing and observed temperature change. *J Geophys Res* 113:D23105. doi:[10.1029/2008JD010405](https://doi.org/10.1029/2008JD010405)
- Gregory JM, Stouffer RJ, Raper SCB, Stott PA, Rayner NA (2002) An observationally based estimate of the climate sensitivity. *J Clim* 15(22):3117–3121. doi:[10.1175/1520-0442\(2002\)015<3117:AOBEO>2.0.CO;2](https://doi.org/10.1175/1520-0442(2002)015<3117:AOBEO>2.0.CO;2)
- Hansen J, Sato M, Ruedy R (1997) Radiative forcing and climate response. *J Geophys Res* 102:6831–6864. doi:[10.1029/96JD03436](https://doi.org/10.1029/96JD03436)

- Hansen J, Nazarenko L, Ruedy R, Sato M, Willis J, DelGenio A, Koch D, Lacis A, Lo K, Menon S, Tsvetkov T, Perlwitz J, Russell G, Schmidt GA, Tausnev N (2005) Earth's energy imbalance: confirmation and implications. *Science* 308:1431–1435. doi:[10.1126/science.1110252](https://doi.org/10.1126/science.1110252)
- Hansen J, Ruedy R, Sato M, Lo K (2010) Global surface temperature change. *Rev Geophys* 48:RG4004. doi:[10.1029/2010RG000345](https://doi.org/10.1029/2010RG000345)
- Hansen J, Sato M, Kharecha P, von Schuckmann K (2011) Earth's energy imbalance and implications. *Atmos Chem Phys* 11:13421–13449. doi:[10.5194/acp-11-13421-2011](https://doi.org/10.5194/acp-11-13421-2011)
- Held IM, Winton M, Takahashi K, Delworth T, Zeng F, Vallis GK (2010) Probing the fast and slow components of global warming by returning abruptly to preindustrial forcing. *J Clim* 23:2418–2427. doi:[10.1175/2009JCLI3466.1](https://doi.org/10.1175/2009JCLI3466.1)
- Hoffert MI, Callegari AJ, Hsieh CT (1980) The role of deep sea heat storage in the secular response to climate forcing. *J Geophys Res* 85:6667–6679. doi:[10.1029/JC085iC11p06667](https://doi.org/10.1029/JC085iC11p06667)
- IPCC (2007) Climate change 2007: the physical science basis. In: Solomon S, Qin D, Manning M (eds) Intergovernmental panel on climate change, Geneva. [http://www.ipcc.ch/publications\\_and\\_data/ar4/wg1/en/contents.html](http://www.ipcc.ch/publications_and_data/ar4/wg1/en/contents.html)
- Ishii M, Kimoto M (2009) Reevaluation of historical ocean heat content variations with time-varying XBT and MBT depth bias corrections. *J Oceanogr* 65:287–299. doi:[10.1007/s10872-009-0027-7](https://doi.org/10.1007/s10872-009-0027-7)
- Jarvis A, Li S (2011) The contribution of timescales to the temperature response of climate models. *Clim Dyn* 36:523–531. doi:[10.1007/s00382-010-0753-y](https://doi.org/10.1007/s00382-010-0753-y)
- Jones GS, Christidis N, Stott PA (2011) Detecting the influence of fossil fuel and bio-fuel black carbon aerosols on near surface temperature changes. *Atmos Chem Phys* 11:799–816. doi:[10.5194/acp-11-799-2011](https://doi.org/10.5194/acp-11-799-2011)
- Joshi M, Shine K, Ponater M, Stuber N, Sausen R, Li L (2003) A comparison of climate response to different radiative forcing in three general circulation models: towards an improved metric of climate change. *Clim Dyn* 20:843–854. doi:[10.1007/s00382-003-0305-9](https://doi.org/10.1007/s00382-003-0305-9)
- Kiehl JT (2007) Twentieth century climate model response and climate sensitivity. *Geophys Res Lett* 34:L22710. doi:[10.1029/2007GL031383](https://doi.org/10.1029/2007GL031383)
- Kloster S, Dentener F, Feichter J, Raes F, Lohmann U, Roeckner E, Fischer-Bruns I (2010) A GCM study of future climate response to aerosol pollution reductions. *Clim Dyn* 34:1177–1194. doi:[10.1007/s00382-009-0573-0](https://doi.org/10.1007/s00382-009-0573-0)
- Knutti R (2008) Why are climate models reproducing the observed global surface warming so well? *Geophys Res Lett* 35:L18704. doi:[10.1029/2008GL034932](https://doi.org/10.1029/2008GL034932)
- Knutti R, Plattner G-K, (2012) Comment on “Why Hasn't earth warmed as much as expected?” by Schwartz et al. 2010. *J Clim* 25:2192–2199. doi:[10.1175/2011JCLI4038.1](https://doi.org/10.1175/2011JCLI4038.1)
- Knutti R, Krähenmann S, Frame DJ, Allen MR (2008) Comment on “Heat capacity, time constant, and sensitivity of Earth's climate system” by S. E. Schwartz. *J Geophys Res* 113:D15103. doi:[10.1029/2007JD009473](https://doi.org/10.1029/2007JD009473)
- Levitus S, Antonov J, Boyer T (2005) Warming of the world ocean, 1955–2003. *Geophys Res Lett* 32:L02604. doi:[10.1029/2004GL021592](https://doi.org/10.1029/2004GL021592)
- Levitus S, Antonov JI, Boyer TP, Locarnini RA, Garcia HE, Mishonov AV (2009) Global ocean heat content 1955–2008 in light of recently revealed instrumentation problems. *Geophys Res Lett* 36:L07608. doi:[10.1029/2008GL037155](https://doi.org/10.1029/2008GL037155)
- Lohmann U, Rotstajn L, Storelvmo T, Jones A, Menon S, Quaas J, Ekman AML, Koch D, Ruedy R (2010) Total aerosol effect: radiative forcing or radiative flux perturbation? *Atmos Chem Phys* 10(7):3235–3246. doi:[10.5194/acp-10-3235-2010](https://doi.org/10.5194/acp-10-3235-2010)
- Lucarini V, Ragone F (2011) Energetics of climate models: net energy balance and meridional enthalpy transport. *Rev Geophys* 49:RG1001. doi:[10.1029/2009RG000323](https://doi.org/10.1029/2009RG000323)
- Lyman JM (2011) Estimating global energy flow from the global upper ocean. *Surv Geophys*. doi:[10.1007/s10712-011-9167-6](https://doi.org/10.1007/s10712-011-9167-6)
- Lyman JM, Johnson GC (2008) Estimating annual global upper ocean heat content anomalies despite irregular in situ ocean sampling. *J Clim* 21:5629–5641. doi:[10.1175/2008JCLI2259.1](https://doi.org/10.1175/2008JCLI2259.1)
- Matthews HD, Caldeira K (2007) Transient climate-carbon simulations of planetary geoengineering. *Proc Natl Acad Sci USA* 104:9949–9954. doi:[10.1073/pnas.0700419104](https://doi.org/10.1073/pnas.0700419104)
- Meehl GA, Washington WM, Wigley TML, Arblaster JM, Dai A (2003) Solar and greenhouse gas forcing and climate response in the twentieth century. *J Clim* 16:426–444. doi:[10.1175/1520-0442\(2003\)016<0426:SAGGFA>2.0.CO;2](https://doi.org/10.1175/1520-0442(2003)016<0426:SAGGFA>2.0.CO;2)
- Meinshausen M, Smith S, Calvin K, Daniel JS, Kainuma M, Lamarque J-F, Matsumoto K, Montzka SA, Raper SCB, Riahi K, Thomson AM, Velders GJM, van Vuuren D (2011) The RCP greenhouse gas concentrations and their extension from 1765 to 2300. *Clim Chang*. doi:[10.1007/s10584-011-0156-z](https://doi.org/10.1007/s10584-011-0156-z)



- Murphy DM, Solomon S, Portmann RW, Rosenlof KH, Forster PM, Wong T (2009) An observationally based energy balance for the Earth since 1950. *J Geophys Res* 114:D17107. doi:[10.1029/2009JD012105](https://doi.org/10.1029/2009JD012105)
- Myhre G, Highwood EJ, Shine KP, Stordal F (1998) New estimates of radiative forcing due to well mixed greenhouse gases. *Geophys Res Lett* 25:2715–2718. doi:[10.1029/98GL01908](https://doi.org/10.1029/98GL01908)
- Myhre G, Myhre A, Stordal F (2001) Historical evolution of radiative forcing of climate. *Atmos Environ* 35:2361–2373. doi:[10.1016/S1352-2310\(00\)00531-8](https://doi.org/10.1016/S1352-2310(00)00531-8)
- Padilla LE, Vallis GK, Rowley CW (2011) Probabilistic estimates of transient climate sensitivity subject to uncertainty in forcing and natural variability. *J Clim* 24:5521–5537. doi:[10.1175/2011JCLI3989.1](https://doi.org/10.1175/2011JCLI3989.1)
- Palmer MD, Haines K, Tett SFB, Ansell TJ (2007) Isolating the signal of ocean global warming. *Geophys Res Lett* 34:L23610. doi:[10.1029/2007GL031712](https://doi.org/10.1029/2007GL031712)
- Palmer M, Antonov J, Barker P, Bindoff N, Boyer T, Carson M, Domingues C, C. SG, Gleckler P, Good S, Gouretski V, Guinehut S, Haines K, Harrison DE, Ishii M, Johnson G, Levitus S, Lozier S, Lyman J, Meijers A, Schuckmann Kv, Smith D, Wijffels S, Willis J (2010) Future observations for monitoring global ocean heat content. In: Hall J, Harrison DE, Stammer D (eds) Proceedings of the “OceanObs’09: Sustained ocean observations and information for society” Conference (vol 2), Venice, Italy, 21–25 September 2009. ESA Publication WPP-306. doi:[10.5270/OceanObs09.cwp.68](https://doi.org/10.5270/OceanObs09.cwp.68)
- Pilewskie P (2011) Measurements of solar spectral irradiance. ISSI Workshop on Observing and Modeling Earth’s Energy Flows. Bern, 10–14 January 2011
- Scafetta N (2008) Comment on “Heat capacity, time constant, and sensitivity of Earth’s climate system” by S. E. Schwartz. *J Geophys Res* 113:D15104. doi:[10.1029/2007JD009586](https://doi.org/10.1029/2007JD009586)
- Schwartz SE (2004) Uncertainty requirements in radiative forcing of climate change. *J Air Waste Manag Assoc* 54:1351–1359. doi:[10.1080/10473289.2004.10471006](https://doi.org/10.1080/10473289.2004.10471006)
- Schwartz SE (2007) Heat capacity, time constant, and sensitivity of Earth’s climate system. *J Geophys Res* 112(D24):D24S05. doi:[10.1029/2007JD008746](https://doi.org/10.1029/2007JD008746)
- Schwartz SE (2008a) Reply to comments by G. Foster et al., R. Knutti et al., and N. Scafetta on “Heat capacity, time constant, and sensitivity of Earth’s climate system”. *J Geophys Res* 113:D15105. doi:[10.1029/2008JD009872](https://doi.org/10.1029/2008JD009872)
- Schwartz SE (2008b) Uncertainty in climate sensitivity: causes, consequences, challenges. *Energy Environ Sci* 1:430–453. doi:[10.1039/B810350J](https://doi.org/10.1039/B810350J)
- Schwartz SE, Charlson RJ, Kahn RA, Ogren JA, Rodhe H (2010) Why hasn’t Earth warmed as much as expected? *J Clim* 23:2453–2464. doi:[10.1175/2009JCLI3461.1](https://doi.org/10.1175/2009JCLI3461.1)
- Smith TM, Reynolds RW, Peterson TC, Lawrimore J (2008) Improvements to NOAA’s historical merged land–ocean surface temperature analysis (1880–2006). *J Clim* 21:2283–2296. doi:[10.1175/2007JCLI2100.1](https://doi.org/10.1175/2007JCLI2100.1)
- Stevens B, Schwartz SE (2012) Observing and modeling Earth’s energy flows. *Surv Geophys*. doi:[10.1007/s10712-012-9184-0](https://doi.org/10.1007/s10712-012-9184-0)
- Sutton P, Roemmich D (2001) Ocean temperature climate off north-east New Zealand. *N Z J Marine Freshw Res* 35:553–565. doi:[10.1080/00288330.2001.9517022](https://doi.org/10.1080/00288330.2001.9517022)
- Takemura T, Tsushima Y, Yokohata T, Nozawa T, Nagashima T, Nakajima T (2006) Time evolutions of various radiative forcings for the past 150 years estimated by a general circulation model. *Geophys Res Lett* 33:L19705. doi:[10.1029/2006GL026666](https://doi.org/10.1029/2006GL026666)
- Watterson G, Dix MR (2005) Effective sensitivity and heat capacity in the response of climate models to greenhouse gas and aerosol forcings. *Q J R Meteorol Soc* 131:259–279. doi:[10.1256/qj.03.232](https://doi.org/10.1256/qj.03.232)
- Webb MJ, Senior CA, Sexton DMH, Ingram WJ, Williams KD, Ringer MA, McAvaney BJ, Colman R, Soden BJ, Gudgel R, Knutson T, Emori S, Ogura T, Tsushima Y, Andronova N, Li B, Musat I, Bony S, Taylor KE (2006) On the contribution of local feedback mechanisms to the range of climate sensitivity in two GCM ensembles. *Clim Dyn* 27:17–38. doi:[10.1007/s00382-006-0111-2](https://doi.org/10.1007/s00382-006-0111-2)
- Willis JK, Roemmich D, Cornuelle B (2004) Interannual variability in upper ocean heat content, temperature, and thermocline expansion on global scales. *J Geophys Res* 109:C12036. doi:[10.1029/2003JC002260](https://doi.org/10.1029/2003JC002260)